Robustness of radiation beam profile measurements

Master's Thesis, 26.5.2023

Author:

Topi Nykänen

Supervisor:

Sami Rinta-Antila
Eeva Boman (TAUH)

UNIVERSITY OF JYVÄSKYLÄ
DEPARTMENT OF PHYSICS

Abstract

Nykänen, Topi
Robustness of megavoltage photon beam profile measurements
Master's thesis
Department of Physics, University of Jyväskylä, 2023, 78 pages.

In this master's thesis, profile measurements of PTW Semiflex 3D and PTW Semiflex ionisation chambers in addition to IBA MatriXX matrix detector were compared to each other using different measurement set-ups. The ionisation chamber measurements were done in a water phantom in horizontal and vertical orientations. Two different set ups were used in the horizontal orientation. The first horizontal set-up used in the current clinical quality assurance program of the radiation therapy clinic at Tampere University Hospital with the wire of the chamber lying deep in the water phantom. The second horizontal measurements were done with more of the wire in the radiation field by having the wire closer to the surface of the water. Measurements were done with 6, 10 and 15 MV photon fields. Flattened fields were measured with 6 and 15 MV energies. Flattening filter free fields were measured for the 6 and 10 MV fields. Field size was set to 20x20 cm^2. All of the measurements were repeated with adding 5° wedge in the radiation beam.

Symmetry, flatness and width of left and right penumbras were compared between the measurements. The symmetry and flatness of the vertically orientated ionisation chamber were in agreement with the matrix detector measurements for all energies and for the open and wedge fields. Vertical Semiflex 3D was similar in symmetry and flatness with horizontal and vertical Semiflex. Horizontally orientated Semiflex 3D deviated significantly on the x-axis from the other measurements in symmetry and flatness. The same effect was not seen on the y-axis. The amount of wire in the radiation field did not affect the measured profiles. Due to the observations that were made, orientation of the ionisation chamber was changed to vertical in the radiation therapy quality assurance program in the clinic.

Keywords: Radiation therapy, beam profile measurement, photon beam, x-ray

Tiivistelmä

Nykänen, Topi
Robustness of megavoltage photon beam profile measurements
Pro gradu -tutkielma
Fysiikan laitos, Jyväskylän yliopisto, 2023, 78 sivua

Tässä pro gradu -tutkielmassa vertailtiin PTW Semiflex 3D ja PTW Semiflex ionisaatiokammioiden sekä IBA MatriXX matriisidetektorin profiilimittauksia eri ionisaatiokammion asetteluilla. Ionisaatiokammio mittaukset tehtiin vesifantomissa vaaka- ja pystyasennoissa. Vaaka-asennossa mittaukset tehtiin kahdella mittausasetelmalla. Ensimmäinen vaaka asettelu tehtiin Tampereen Yliopistollisen Sairaasalan sädehoitoyksikön kliinisen laadunvalvontaohjelman mukaisesti, siten että kammion johto upotettiin syvälle vesifantomiin. Toisessa vaaka asettulussa suurempi osa johdosta jätettiin säteilykeilaan vetämällä johto lähemmäksi veden pintaa. Mittaukset tehtiin 6, 10 ja 15 MV: fotonikentille. Tasoitetuille kentille mittaukset tehtiin 6 ja 15 MV:n energioilla. Tasoittamattomattomat kentät mitattiin 6 ja 10 MV:n energioilla. Kentänkoko asetettiin 20x20 cm^2:n. Kaikki mittaukset toistettiin lisäämällä 5° kiila säteilykenttään.

Säteilykenttien profiileista vertailtiin symmetriaa, tasaisuutta ja puolivarjojen leveyttä. Pystyyn asetettu ionisaatiokammio vastasi matriisia symmetriassa ja tasaisuudessa kaikilla energioilla ja kiilan olessa säteilykentässä. Pystyyn asetettu Semiflex 3D vastasit symmetriassa ja tasaisuudessa Semiflex ionisaatiokammiota. Vaakaan asettu Semiflex 3D erosi muista mittausasetteluista x-akselilla symmetriassa ja tasaisuudessa huomattavasti. Y-akselin suuntaisissa profiileissa ei havaittu samaa efektiä. Ionisaatiokammion johdon määrä säteilykentässä ei vaikkuttanut mitattuihin profiileihin. Tässä tutkimuksessa saatujen tulosten perusteella sädehoitoyksikön laadunvalvontaohjelmassa ionisaatiokammion asettelu vaihdettiin pystyyn.

Avainsanat: Sädehoito, profiilimittaus, sädehoitokenttä, fotonisäde, röntgensäde

Preface

Gradun tekeminen Tampereen yliopistolliseen sairaalaan sai yhden unelman täytymään tämän lukuvuoden aikana. Kiitos Eevalle aiheesta ja ohjauksesta. Gradun ja sairaala Novaan tehdyn erikoistyön avulla sain erikoistuvan fyysikon paikan kesäksi sairaala Novasta, mikä täytti jo toisen unelman. Kiitos myös Samille gradun ohjaamisesta. Kiitos Tuomakselle erikoistyöstä ja työpaikaista. Edelliset viisi vuotta ovat olleet melko raskaat opiskeluiden ulkopuolella. Viimeinen ja suurin kiitos täytyy antaa äidilleni kaikesta tuesta opintojen ulkopuolella, ilman sitä tämä ei olisi ollut mahdollista.

Jyväskylä 26.5.2023

Topi Nykänen

Contents

Abbreviations

AAPM - American Association of Physicists in Medicine

CT - Computed tomography

CTV - Clinical target volume

DNA - Deoxyribonucleic acid

FWHM - Full width half maximum

FFF - Flattening filter free

GTV - Gross tumour volume

IAEA - International Atomic Energy Agency

IEC - International Electrotechnical Commission

IMRT - Intensity modulated radiation therapy

ITV - Internal treatment volume

MLC - Multi-leaf collimator

MV - Megavoltage

PDD - Percentage depth dose

PTV - Planning target volume

QA - Quality assurance

RCF - Radiochromic film

SSD - Source-to-surface distance

STUK - Radiation and nuclear safety authority (Säteilyturvakeskus)

TAUH - Tampere University Hospital

TG - Task group

VMAT - Volumetric modulated arc therapy

1 Introduction

To understand how radiation therapy works and why radiation safety is important, knowledge of some basic biology is required. Irradiation can have multiple effects on cells [1, p. 489]. The irradiation can have no effect at all, it can delay cell division or cause apoptosis (programmed cell death). Reproductive failure and genomic instability cause cell to die during cell division. Cells can survive but contain mutations, which can lead to transformation in cell phenotype. Genetic damage in cells can also be caused by bystander effect, which cause irritated cells to send signal to surrounding cells that lead to genetic changes in their DNA. Cell can also adapt to the radiation which leads to them becoming more resistant to radiation.

In radiation therapy the goal is to kill all of the cancerous cells in a target area, so that the the cancer does not renew locally [2]. To ensure the high accuracy of radiation therapy treatments, quality assurance (QA) program is performed routinely in the radiation therapy clinic according to safety guidelines set by the authorities. QA measurements include safety and performance checks carried out in a specific time intervals. Each radiation therapy clinic sets their own QA program, but usually international and national guidelines are followed. [1] In Finland the regulations regarding the use of radiation are set in the Radiation act 859/2018 [3], which authorises the Radiation and nuclear safety authority (STUK) to set regulation regarding the safe use of radiation. STUK regulation S/5/2019 [4] gives instructions on radiation safety in the use of radiation sources and devices. Radiation act and regulation S/5/2019 give the requirements on radiation use in medical applications. Guidelines for decommissioning radiation sources from use are included in regulation S/5/2019.

The goal of this masters thesis research was to see if changing the orientation of an ionisation chamber would cause differences in measured photon beam profile characteristics. Horizontal and vertical positioning of the ionisation chamber were compared to each other. In the horizontal position the wire of the chamber was routed in two different ways into the water tank. This was done to see if having more of the wire in the field exposed to the radiation beam would cause affect the

measured ionisation current. The profiles were also measured with a matrix detector in two different orientations. The measured matrix profiles were compared to the ionisation chamber measurements. All measurements were repeated with a 5° wedge. Four different photon beams were measured with energies between 6 and 15 MV. Ionisation chamber measurements were done PTW (PTW Dosimetry, Germany) Semiflex 3D in a PTW BEAMSCAN water phantom. IBA (IBA dosimetry Gmbh, Germany) MatriXX was used as the matrix detector.

2 Overview of radiation therapy

2.1 Production of megavoltage photons

In the megavoltage (MV)[1] range, the produced radiation beam is called a photon (x-rays for example) beam. In external beam photon therapy the patient is treated with a photon beam. This beam is produced by accelerating electrons. The electron beam hits a target that is usually made out of a heavy metal. The target is usually made of tungsten, which is used because of its high atomic number (Z=74) and melting point of 3370 °C. [5]

Interactions between the electrons and the target material produce photons, which are emitted as a result of characteristic and Bremsstrahlung interactions. Bremsstrahlung interaction is the main interaction in the MV energy range. Photons produced by the Bremsstarhlung interaction have continuous[2] energy spectrum, which means the emitted photons can have any energy between zero and the kinetic energy of the electron. As an electron collides with a nucleus of an atom the direction of the electron changes. In this coulomb interaction the electron can loose all or some of its kinetic energy. This change in kinetic is energy emitted as a photon. [5]

Measured doses are often presented as a percentage depth dose (PDD) curve. Figure 1 shows PDD curves for Co-60 γ-rays and different photon beams. [1, 5] Depth at which the maximum dose D_{max} is achieved is called the depth dose maximum which gets increaes with increasing energy. In figure 1, the depth dose maximums are between 0.5 to 5 cm. In dose depth curve, the region from the surface of the water z_0 to dose depth maximum z_{max} is called buildup region.

[1] For photon beams kV and MV are used to denote energy of the beam. keV and MeV are used for electron beams.

[2] Characteristic photons have specific energies.

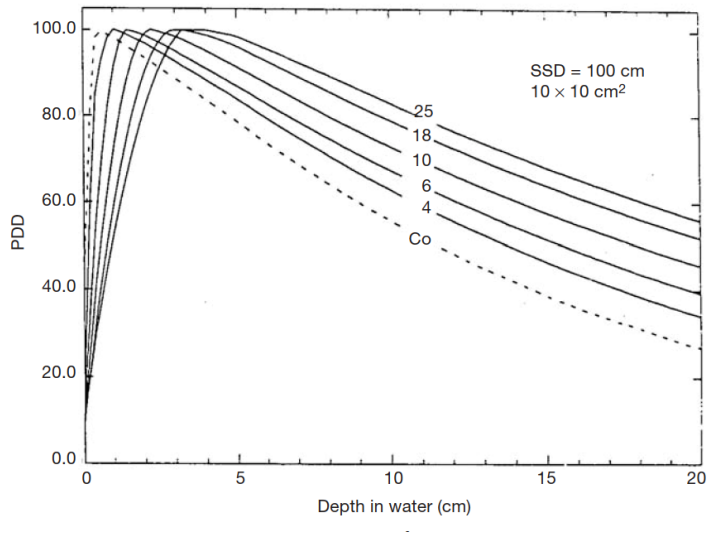

Figure 1. Co-60 γ-ray and x-ray PDD curves for a 10x10 cm^2 field. X-ray curves are shown at 4, 6, 10, 18 and 25 MeV energies. Co-60 γ-ray energy is 1.17 and 1.33 MV. [1, p. 182]

2.2 Photon interactions

In a medium, the photons interact in multiple different ways. Photon interactions are coherent (Rayleigh) scattering, photoelectric effect, Compton effect and pair production. In coherent scattering, the photons change direction when they collide with atoms of the medium without energy losses. Coherent scattering is negligible in radiation therapy because its probability is low in low atomic number materials. [5, p. 62]

Photoelectric effect causes an electron to be emitted from the atom, which creates characteristic x-rays, and can create Auger (secondary) electrons. When a photon collides with an atom its kinetic energy is absorbed by the collision by the atom. The collision causes the atom to emit an electron, which leaves a vacant electron state. The atom is then in an excited state that gets released when an electron on a higher state fills the vacancy by emitting a photon. The emitted photon can be absorbed by an electron in the atom creating an Auger (secondary) electron to be emitted. [5, p. 63]

Compton effect is an interaction between a photon and an electron that has a small (near zero) binding energy [5, p. 64]. After the collision the photon changes its direction and loses some of its kinetic energy to the electron, causing the electron

to be emitted from the atom. Energies of the scattered photon and electron follow equations (1) and (2). As can be seen from figure 3, Compton effect is the dominant interaction in MV photon radiaition therapy, which commonly uses photon energies that are between 5–10 MV. Photoelectric effect is dominant at lower energies in low atomic number materials.

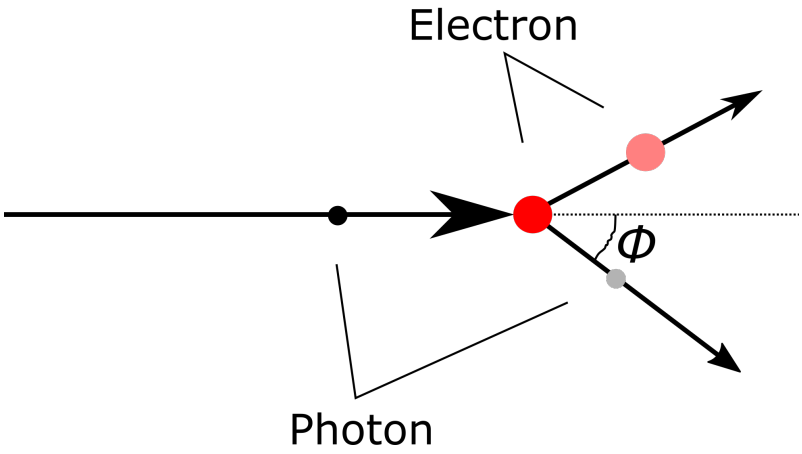

Figure 2. Diagram of the incoming photon colliding with an electron in Compton effect. Angle ϕ is the scattering angle of the photon after the collision.

$$E_e = hf_0 \frac{\alpha(1 - cos\phi)}{1 + \alpha(1 - cos\phi)} \tag{1}$$

$$E_p = hf' = hf_0 \frac{1}{1 + \alpha(1 - cos\phi)} \tag{2}$$

In equations (1) and (2), hf_0 is the energy of the photon before the collision, constant $\alpha = hf_0/m_e c^2$, where $m_e c^2$ is the rest mass energy of an electron (0.511 MeV). Angle ϕ the scattering angle for the photon relative to the incoming photon.

If the photons energy is over 1.02 MeV, the collision with an atom can result in pair production. The photon interacts with the nucleus of an atom that then emits an electron and a positron. Both have a rest energy of 0.511 MeV. This gives the minimum energy requirement for the photon energy. The energy that exceeds 1.02 MeV is given to the particles as kinetic energy. [1, 5] When photon energies are

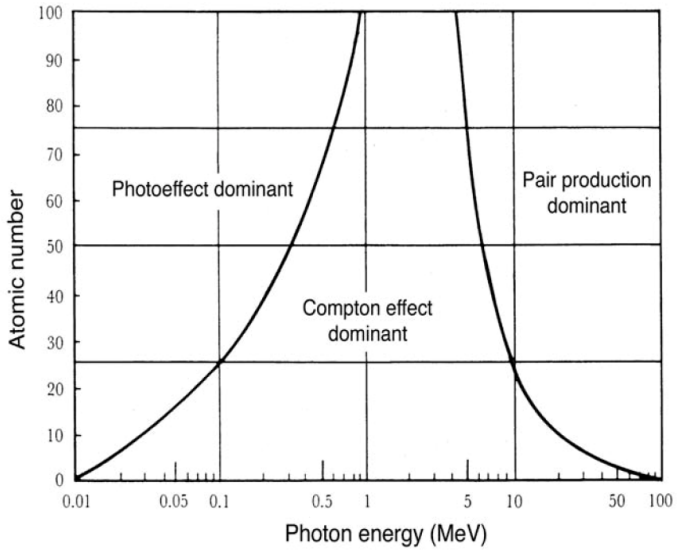

Figure 3. Atomic number as a function of photon energy that shows which effects are dominant in different conditions. At low photon energies photoelectric effect is dominant. With photon energies between 1–10 MV Compton effect is dominant. [1, p. 37]

below 10 MV in low atomic number materials pair production is only up a small portion of the photon interactions (Figure 3).

2.3 Biology of radiation therapy

Photons cause cell damage directly and indirectly in interactions with the atoms in tissues [1, p. 488-489]. Photons can interact directly with tissues, which causes ionisations and excitations in the tissues. Indirectly high energy photons cause damage in cells in four steps. In the first step, a photon interacts in a medium producing free high energy electrons. These electrons then create free radicals[3] in water in the second step. Free radicals break chemical bonds in DNA which can lead to biological effects associated tissues. Photons cause about two thirds of cell damage indirectly.

Radiation effects are deviated into deterministic and stochastic effects [1, p.550-551]. Deterministic effects happen at certain dose levels and are evident shortly after exposure. High doses cause nausea, skin reddening and can cause loss in tissue functions. Source of deterministic effects are cell death and delayed cell division.

[3] H_2O^+ (water ion) and OH• (hydroxyl radical)

Effects that become evident after a longer period of time are called stochastic effects. Mutations caused by radiation can for example cause cancer or hereditary effects due to mutations in germ cell.

2.4 Radiation therapy treatment planning

For radiation therapy each patient is having an individual treatment plan, which usually uses a three dimensional computed tomography (CT) image. The treatment plan is then done by defining the target volumes to the CT-images. Typical target volumes are shown in figure 4. Gross tumour volume (GTV) includes the visible location of the tumour. Clinical target volume (CTV) contains the GTV and the surrounding areas that could have microscopic parts of the tumour, which have to be treated to go into recovery. Around the CTV is ITV that is there to take into account the movements and size variations of different organs around the tumour. In addition, the error margins of the treatment machine, patient positioning uncertainties and in-treatment variations are included in the planning treatment volume (PTV) that surrounds the ITV. Healthy tissues around the tumour are also marked in the treatment plan, so that the dose in the healthy tissues can be minimised. [1, p. 219–222]

Radiation therapy treatments are typically given in fractions and treatments take multiple weeks. Fractionation schemes are based on five R's of radiotherapy: Radiosensitivity, Repair, Repopulation, Redistribution and Reoxygenation. All cells in different tissues have differing radiosensitivities. Cells can repair sublethal damage caused to them by radiation. Cells can reproduce and repopulate during treatments. Distribution changes in different stages of the cell cycle their sensitivity varies as the fractions are given. Hypoxic cells go through reoxygenation which decreases their resistance to radiation. Commonly treatment fractions are given on five days a week over multiple weeks. By fractioning damage to healthy tissues can be reduced because the healthy cells repair their DNA more efficiently from sublethal damage than the cancer cells. The normal tissues also have a chance to repopulate between fractions. [1, p. 501-502]

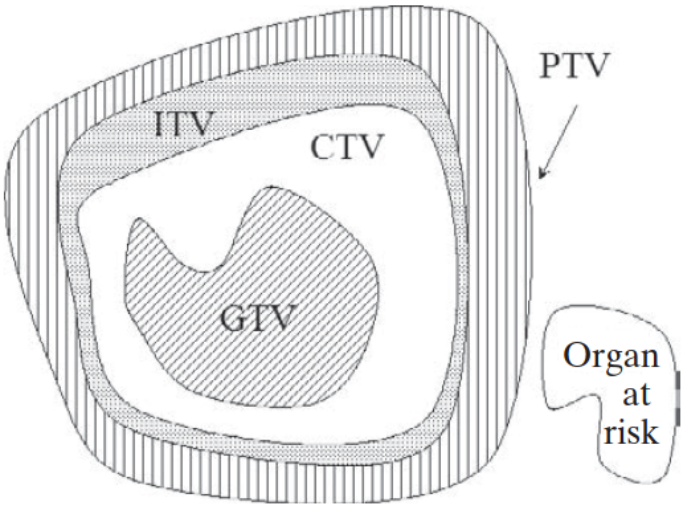

Figure 4. Volumes of interest which labelled into the treatment plan. Healthy tissues which are at risk of being radiated are also labelled. GTV = Gross tumour volume, CTV = Clinical target volume, ITV = Internal target volume, PTV = Planning target volume. [1, p. 220]

2.5 Linear accelerator (Linac)

Linear accelerators, commonly called linacs, are the treatment machines used in radiation therapy to accelerate particles and produce high energy beams. Currently there are two main manufactures for radiation therapy treatment machines Varian medical systems (USA) and Elekta (Sweden). Electrons are shot into an accelerator tube from an electron gun. Electromagnetic waves produced by a magnetron or a klystron accelerate the particles in the tube. [5]

From the accelerator tube the beam enters treatment head. In most machines, the beam needs to be turned. In Varian's treatment machines, this is done turning the beam 270° with three magnets. Each magnet turns the beam 90° (Figure 5b). Other manufacturers have used 90° and 112.5° bends. Some[4] treatment machines have the accelerator tube inside the treatment head pointing down, in which case the there is no need to turn the beam. [1, 5]

Modern treatment machines have three different types of collimators (Figure 6). Primary, secondary and multi-leaf collimators. The primary collimator is fixed in place and sets the maximum field size. Field size is limited by the secondary

[4]Accuray Cyberknife for example

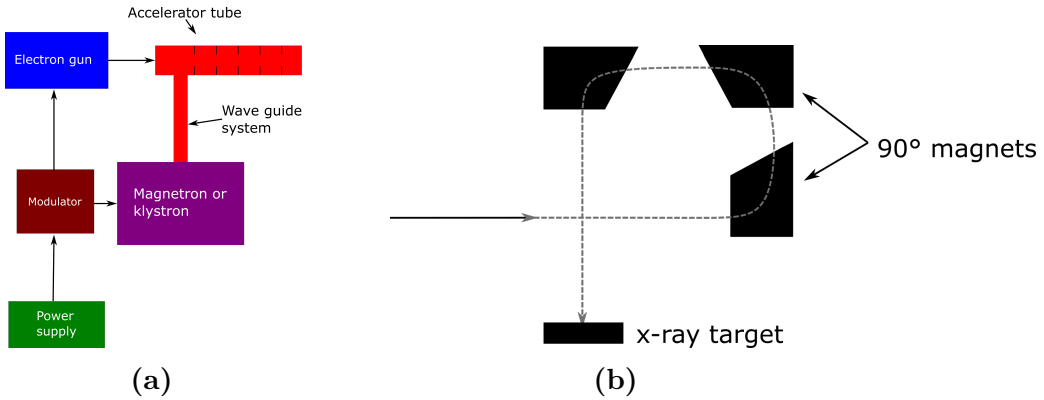

Figure 5. (a) Sketch treatment linac structure. Electron gun shoots electrons into the accelerator tube. A magnetron or a klystron creates electromagnetic waves into the accelerator tube. Modulator transforms the power supplies DC voltage into DC pulses. The diagram was adapted from [5, p. 43]. (b) Accelerated electron beam needs to be turned 90° downwards. The beam is usually turned 270° in 90° increments.

collimators during treatments. The secondary collimators can move during treatments in modern treatment machines. Multi-leaf collimators (MLC) can change the field shape of the treatment field during treatments to be more irregular. MLCs usually have 60 to 80 pairs of the so called leaves. The leaves are usually made of tungsten. Each leaf is 0.25–1 cm wide and 6–7.5 cm thick. The arrangement of the MLC can be changed during treatments so that dose in healthy tissues around treatment area can be decreased and direct the dose precisely to the tumour. Intensity modulated radiation therapy (IMRT) and volumetric modulated arc therapy (VMAT) are technologies that use MLC's to modulate the beam during treatments. [5, 6]

Photon beam intensity profile can be flattened by using a flattening filter (Figure 7). The filter is made of a high atomic number material. While treating a patient the beam is flat at a certain depth. In some cases, this can cause the field to have so called horns at shallow depths which are visible in the larger 30x30 cm^2 fields of figure 7. The smaller 10x10 cm^2 fields do not have these horns in figure 7. [1, 2]

Treatment machines allow the flattening filter to be moved aside. This how a flattening filter free (FFF) beam is formed. Figure 8 shows a 6 MV photon beam profile with and without a flattening filter. The beam intensity is higher on the central axis of the beam and lower at the edges. Intensity modulated radiation therapy (IMRT) and volumetric modulated arc therapy (VMAT) technologies have made therapeutic use of FFF fields possible. Dose rates can be much higher in

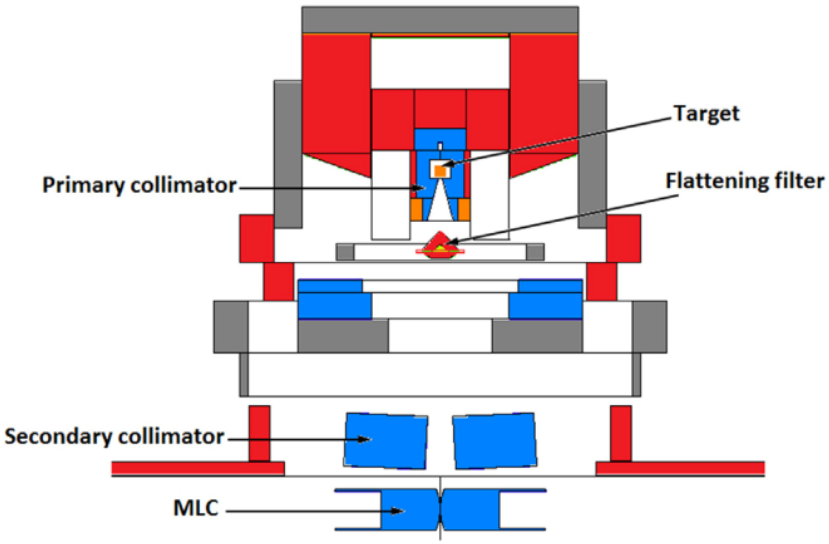

Figure 6. Structure of the treatment head of a treatment machine. Components are colour coded by the metal they are made of. Red = iron, orange = copper, gray = lead, blue = tungsten and yellow = tungsten. [6]

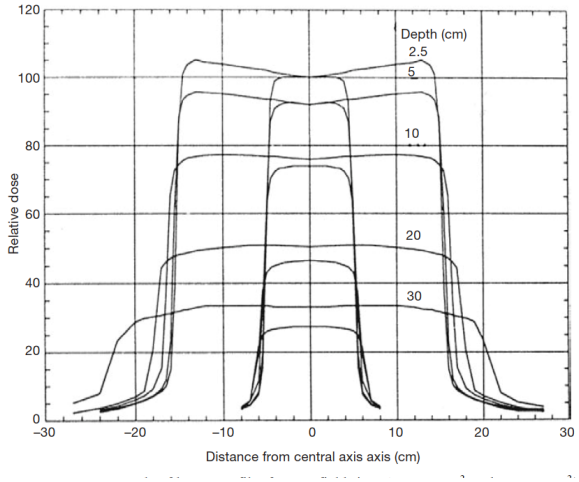

Figure 7. Profiles for 10x10 cm^2 and 30x30 cm^2 10 MV photon beams. The relative dose of the beam at different depths are presented in the figure. [1, p. 195]

FFF fields than in flattened fields. [5, p. 173–176] The flattening filter lowers the maximum intensity of the beam significantly. Using a flattening filter reduces the beam intensity by about 50 % and up to 60 % on the central axis for a 10 MV photon beam. [7, 8]

Flattened fields have a higher neutron dose [8]. Photon interactions with high atomic number materials emit neutrons. Primary collimator, target, flattening filter,

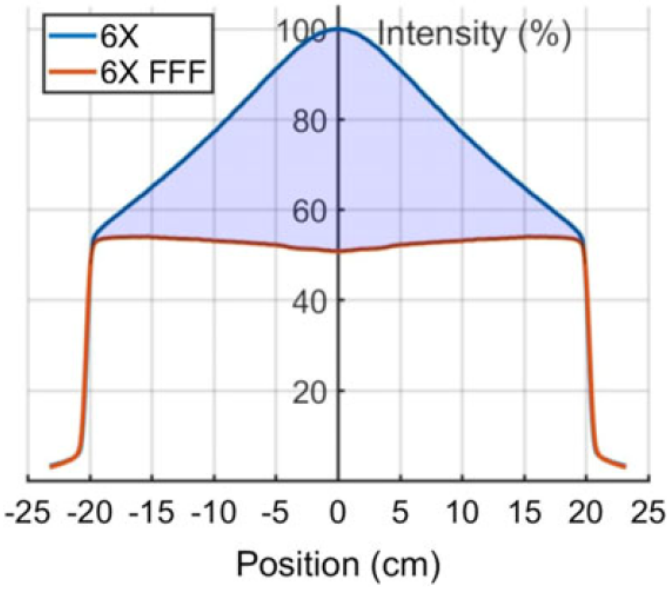

Figure 8. A flattened and flattening filter free (FFF) radiation field profile for a 6 MV photon beam. The figure shows the difference in beam intensity in the field. The FFF field has much higher intensity especially along the central axis of the field. [7] Correction: Blue is the 6FFF beam and red the 6X beam.

jaws and the MLC produce neutrons as photon collisions happen with the treatment machines parts. With photon energies under 10 MV neutron dose is small and can be neglected. When using higher photon energies, the neutron dose is high enough that most radiation therapy clinics do not use photon energies over 15 MV in IMRT or VMAT treatments. [8]

2.6 Radiation beam characteristics

Relative dose profiles for photon field sizes 10x10 cm^2 and 30x30 cm^2 at different depths are shown in figure 7. The profile shows dose around the central line of the beam. Usually, maximum dose is at the central point of the profile, which can be seen in the 10x10 cm^2 field in figure 8. When the field size increases, the relative dose increases on the edges of the beam at shallow depths. This can be seen in the 30x30 cm^2 fields in figure 8. [1, p. 194-196]

Equation 3 is the definition of International Electrotechnical Commission (IEC) for beam symmetry [9]. Symmetry is defined as the maximum quotient of two points

that area equally far from the central axis in the flattened area. In equation (3), Point L and Point R are the dose on the left and right side of the profile.

$$S = 100 \cdot \mathrm{Max}\left(\left|\frac{\mathrm{PointL}}{\mathrm{PointR}}\right|, \left|\frac{\mathrm{PointR}}{\mathrm{PointL}}\right|\right) \tag{3}$$

IEC defines beam flatness with equation (4). Maximum dose D_{max} is anywhere in the field. minimum dose D_{min} in the flattened area of the beam. [9]

$$F = 100 \cdot \mathrm{Max}\left(\frac{D_{max}}{D_{min}}\right) \tag{4}$$

Penumbra is the region at the edge of the profile where the beams dose plummets as a function of distance from the central line of the profile. It consists of transmission, geometric and physical penumbra. Photon transmission through the collimator causes the transmission penumbra. It can be made smaller by having the collimator edges be in line with the edge of the beam. Geometric penumbra is dependant on the diameter of the electron beam. Distance from source-to-surface (SSD) affects the size of the geometric penumbra. Scattering of photons in tissues creates a physical penumbra. Lateral width of the physical penumbra is determined from 20–80 % isodose levels (Figure 9). [1, 5, 10]

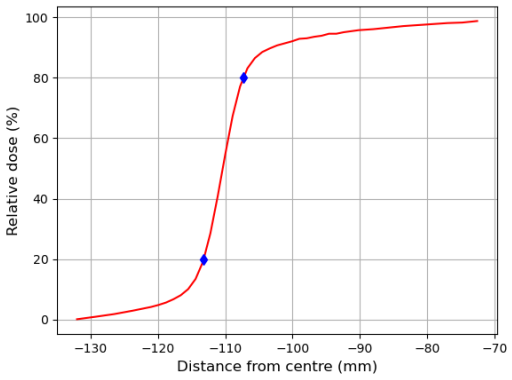

Figure 9. The blue diamonds show the 20 and 80 % relative dose points on the left side of the beam.

Absorbed dose D (Equation 5) is the amount of energy that radiation energy dE that was transferred to a medium with a certain finite mass dm [1, p. 49]. Unit is either in J/kg or Gy (gray). Photons ionise indirectly, as photons interact in tissues the interactions produce charged particles. These charged particles cause the absorbed dose into the tissues.

$$D = \frac{dE}{dm} \tag{5}$$

Measured doses are commonly presented as percentage depth dose (PDD) curves. PDD (Equation 6) is used to present dose D_z at a certain depth as a portion of the

maximum dose D_{max} at the dose depth maximum depth z_{max}. Figure 1 depicted the PDD curves of photon beams with different energies and Co-60 γ-ray beam. [1]

$$PDD = 100\% \cdot \frac{D_z}{D_{max}} \tag{6}$$

The region between zero and the maximum D_{max} is called the buildup region. The dose depth maximum z_{max} of the the beam is deeper for higher-energy beams. Lower-energy beams have higher skin-doses as the D_{max} is closer to the skin surface, because of the larger buildup region higher-energy beams have a skin-sparing effect as the z_{max} is deeper. [5] In the buildup region, photons produce free electrons into the tissues that travel deeper. The electrons release their energy significantly deeper from their origin. Because of this the electron fluence grows until the dose depth maximum is reached.

3 Typical detectors

3.1 Ionisation chambers

Photons cause ionisations in different molecules while travelling in air. In an electric field between two plates, positive ions travel towards the negative plate and negative ions towards the positive plate producing a current flow in the circuit. This ionisation current can be measured with an electrometer. In free air ionisation chamber, outside of the chamber volume and some photons carry their energy to the chamber volume. This needs to be compensated by taking these extra ionisations produced outside the chamber volume, which travel into the chamber volume. Free-air ionisation chambers are mostly used in standardising laboratories. Closed ionisation chambers are more practical to use in QA measurements than free-air ionisation chambers, because of their size and ease of use. Closed thimble[5] (cylindrical) chambers are commonly used in radiation therapy dose measurements. [1, 5]

One type of cylindrical chamber is a Farmer type ionisation chamber (Figure 10), which have three electrodes that are an outer, central electrode (collector) and a guard electrode. Outer electrode also works as the thimble's wall that is either made from graphite or plastic. Different plastics are used to resemble different mediums. For example air- and tissue-equivalent plastics are used. High-energy photons cause outer electrode to ionise. This produces free-electrons into the air cavity which travel to the central electrode. Central and guard electrodes are held at positive a high voltage with the electrometer. The central electrode collects negative charges. Outer electrode is at ground potential. Guard electrode wraps around the central collector and is surrounded by an insulator. The guard electrode keeps charge leakage from away from the central electrode. The insulator is there to insulate the guard from the outer electrode. In typical Farmer type ionisation chamber, the volume of the chamber is 0.6 cm^3. [1, 5]

The Semiflex (PTW) and Semiflex 3D (PTW) ionisation chambers have similar structures and function in the same way as the Farmer type chamber. Both of the

[5]Comes from the sewing thimble like shape of the detectors tip

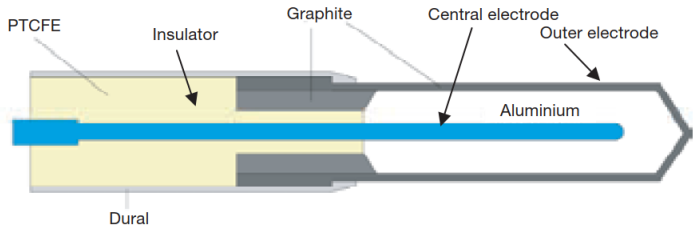

Figure 10. Structure of a Farmer type ionisation chamber. The aluminium central electrode is inside a thin outer electrode. The central electrode works as a collector. The outer electrode surrounds the aluminium collector. Guard electrode is not visible in the image. Guard electrode is in the insulator between the outer and central electrodes. [1, p. 77]

ionisation chambers are smaller than the Farmer type chamber, which makes them more suitable for beam profile measurements as the smaller chambers have a higher measurement resolution. The Semiflex (PTW) has a chamber volume of 0.125 cm^3 and the Semiflex 3D (PTW) has a volume of 0.07 cm^3. [11]

Ionisation chambers output current is usually in piko- to nanoampere range, which is why an electrometer is used to measure the current. [5, 12] The electrometer is a high-impedance operational amplifier. Configuration of the amplifier affects what quantity it measures. [5] Integrate mode op-amp measures the ionisation charge Q that is then shown as a voltage. The charge Q is collected by a capacitor in this configuration. Rate mode measures the ionisation current I directly and converts it into a voltage. Compared to integrate mode op-amp the capacitor is replaced by a resistor. Direct-exposure reading mode can display the direct-exposure reading value R or R/min.

Another type of chamber is a parallel-plate ionisation chamber (Figure 11a), which can be used in surface dose and depth dose measurements for MV photon beams [1, 5]. These ionisation chambers have an entrance window. Opposite to the window is a collector electrode. The entrance window also functions as a polarising electrode and the collector as a guard electrode. The collector electrode, which also acts as the chambers back wall, can be made from conducting plastic or non-conducting material with a thin layer of conducting material on top. Figure 11b shows a commercial parallel-plate chamber Roos chamber (PTW), which has a sensitive volume of 0.35 cm^3.

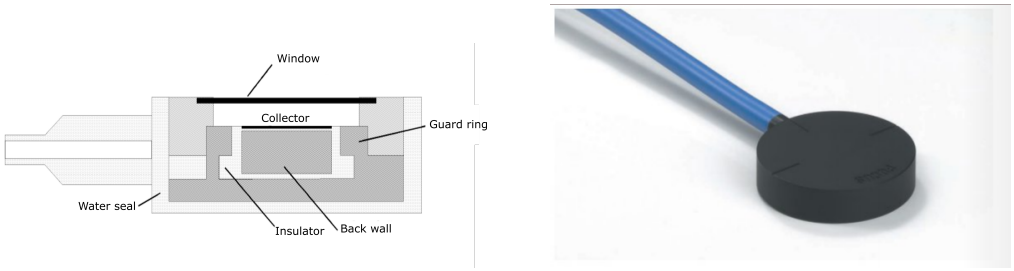

(a) **(b)**

Figure 11. (a) Parallel ion chamber construction. Edited from [12]. (b) Image of PTW Roos Chamber Type 34001. [11]

3.2 Water phantom

Water phantom is used to measure the radiation dose in water. Water sealed chambers are used in the measurements. The phantom can be either home made plexiglass container or commercially sold equipment [5].

Figure 12. PTW BEAMSCAN water phantom positioned under the treatment machine gantry. [13] During the measurements the phantom was positioned as in the image.

The BEAMSCAN (PTW, Germany) is an example of a commercially sold water phantom. The water container of the phantom has 15 mm PMMA walls and dimmensions of 500x500x415 mm [13]. The electrometer is build-in to the phantom, has two channels for the field and reference chambers. Measurement resolution of the electrometer is 10 fA and its measurement range is 2 pA–500 nA and provides

chamber voltages from 0 to ±400 V.

Ionisation chambers are mounted on to the water phantom via TRUFIX (PTW) system. The system has multiple different mounts for the different chambers that are compatible with the BEAMSCAN (PTW) water phantom. The reference detector has its own mount to be mounted in the corner of the phantom.

3.3 Matrix detector

Two dimensional matrix detector device consists of multiple ionisation chambers, at the same depth with equal separation. The matrix detector is used without phantom and requires less set-up time than water phantom measurements with an ionisation chamber. MatriXX (IBA) detector has 1024 air-vented ionisation chambers in a 32 by 32 grid with a separation of 7.62 mm centre-to-centre. Each chamber measures a dose in its location creating a single pixel to the measured two dimensional profile. The structure of the detector is presented in Figure 13. [9, 14, 15]

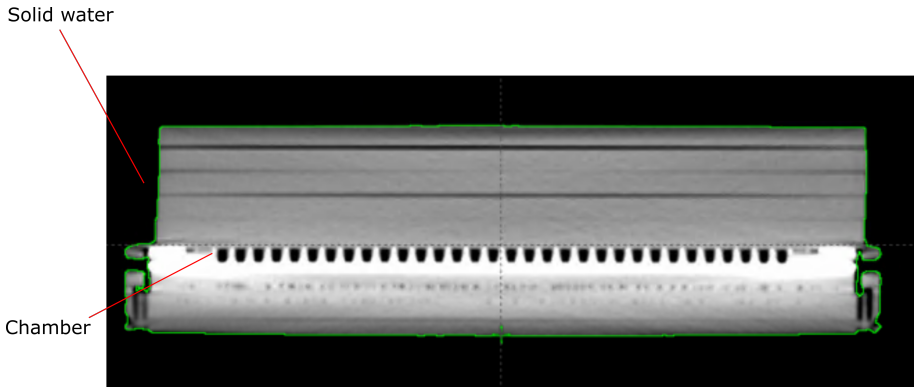

Figure 13. CT image of IBA MatriXX detector shows its internal structure. Ionisation chambers that are inside detector are on top of a copper plate. On top the detector is 5 cm of solid water plates.

Top of the detector is 3 millimeters ABS (Acrylonitrile butadiene styrene) Tecaran. The chambers are on top of a copper plate. The plate is connected to the chambers via their anodes. Below the copper plate there is a 3.5 cm of back-scatter material. A micoroelectronic chip reads every chamber's measurements individually with two different counters. This way both dead time and read-out time between measurements are minimised. The minimum read out time of the device is 20 ms. [9, 14]

3.4 Diode detectors

Diode detectors can be also in dose measurements. Radiating a diode (Figure 14) creates electron-hole pairs. A contact potential causes an electric field in the depletion layer. This causes a current over the diode as electrons and holes move across the diode. This can be converted to the delivered dose by calibrating the detector. Diode detectors do not need a bias voltage as the potential difference over the pn-junction moves the electrons and holes into opposite directions. [2, 16]

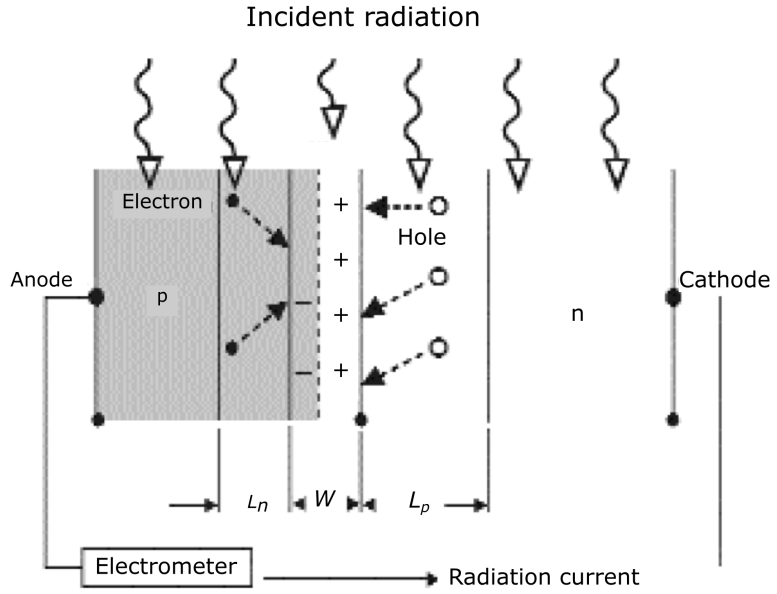

Figure 14. Structure of a diode detector. Radiation generates minority charge carriers in semiconductors. These are excess free holes n-type and excess free electrons in p-type semiconductors. Minority charge carriers that form within the diffusion length (L_n and L_p) on each side of the depletion layer can migrate into the depletion layer. Depletion layer has width W. [16] (Image edited for clarity)

Due to their small size and ease of use diode detectors have been used in the dosimetry measurements during treatments (*in vivo*). Dose measurements during treatments makes it possible to compare the calculated doses in the treatment plan and the delivered doses. This helps in quality assurance (QA) and functions as an additional safety net to limit set up and calculation errors. TG-62 [16] (Task Group 62) gives instructions on how diodes can be used in patient specific *in vivo* QA and dosimetry measurements. Diodes can also be used in water phantom measurements and are well suited for small field dosimetry.

In TRS-483 [17], diodes are recommended for small field measurements. The volume averaging effect of diodes is small as diodes have small sensitive volumes. MicroSilicon (PTW) and Microsilicon X (PTW) [11] are examples of diode detectors. Both detectors have a sensitive volume of 0.03 cm^3. Microsilicon (PTW) is an unshielded diode detector and Microsilicon X (PTW) has a shielded diode. Unshielded diodes have been reported to be better in small field dosimetry.

3.5 Radiographic and radiochromic films

Radiographic and radiochromic films (RCF) are used in radiation therapy QA. AAPM task group reports TG-69 [18] and TG-235 [19] describes their use in dosimetry. Radiographic films are more suitable for electron beams and kilovoltage x-ray beams dosimetry than for megavoltage photon beams.

Radiographic films are commonly made from silver halides (AgH) [18]. These AgH crystals are in an emulsion that is inside a thin polyester layer. Silver bromide (AgBr) and silver iodide (AgI) crystal mixes have been used by Kodak in radiographic films. Radiating the film cause the bromide to ionise and lose its charge. This process is shown in figure 15. The film needs to be processed before the measurement can

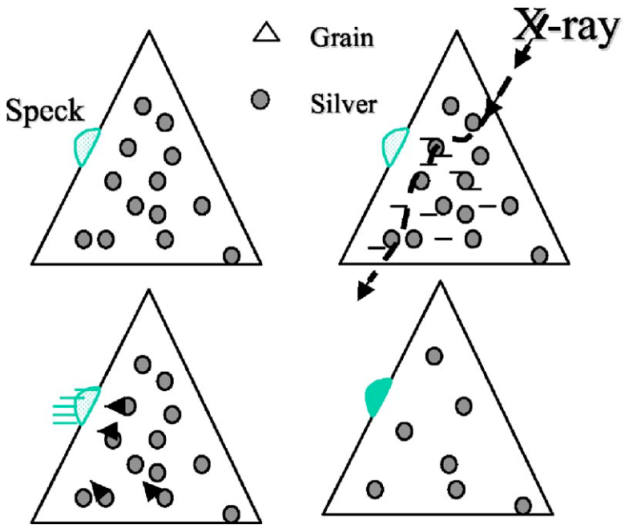

Figure 15. Irritating a AgBr radiochromic film causes with radiation the bromide to ionize. This causes the bromide to lose an electron that move to impurities (specks) in the film, charging them negatively. Positively charged silver ions follow the electrons to the impurities filling them. [18]

be analysed. In processing, the silver grains, that form due to the ionisations, get reduced. This processing is done in four parts: developing, fixing, washing and drying.

RCFs are more suitable in higher dose dosimetry than radiografic films [19]. Multiple different chemical compositions are used to make RCF. Most of the film is hydrogen, oxygen and carbon. The films can also have trace amounts of different elements[6]. Like in radiographic films the radiochromic film is inside a polymer coating.

Radiochromic films can be used in dosimetry for both normal sized fields and small fields. RCFs can be used in dose and profile measurements. For smaller fields some correction factors need to be used to correct measured doses. [19]

To get the absorbed dose from the film optical density (OD) is measured with a densitometer [18]. OD quantifies the amount of light passing through the film. Equation (7) defines optical density as a logarithmic quantity. Light intensity without the film is I_0 and the measured intensity that passes through the film is I.

$$OD = \log_{10} \frac{I_0}{I} \tag{7}$$

[6]Used elements include lithium (L), aluminium (Al), sodium (Na), chloride (Cl) etc.

4 QA and radiation safety in external radiation therapy

4.1 Quality assurance

4.1.1 QA measurements

STUK Guide ST2.1[7] [20] gives recommendation of the measurements to be included in the radiation therapy QA program. Test intervals, methods, instruments and devices that are used in the QA checks should to be included in the QA program. The approval criteria and the following actions that are taken if the approval criteria are not met should be found as well in the QA documentation.

In Finland, STUK regulation S/5/2019 [4] sets tolerances on radiation therapy QA. According to S/5/2019 [4, App. 4] the point dose must not differ more than ±3 % in the reference geometry and must be than ±5 % in the gross tumour volume (GTV) compared to water equivalent phantom measurements. In the reference geometry, repeated phantom measurements should be within 0.5 % of the previous measurement. Further recommendations on radiation safety in radiation therapy are given in STUK Guide ST2.1 [20].

In TG-45 [21] and TG-142 [22], the American Association of Physicists in Medicine (AAPM) gives recommendations on QA measurements in radiation therapy, which are similar with STUK's recommendations. Different beam characteristics are measured regularly to make sure that there are no changes that would risk patient or radiation therapy worker safety. Main properties that QA measurements that monitor beam output include absolute dose, field profiles and depth dose characteristics. AAPM TG-142 also gives recommendations to QA tests to be done daily, monthly or annually. The task group report divides the QA procedures into four categories: dosimetry, mechanical, respiratory gating and safety. Depending on the machine type different tolerances are given in tables I–III on pages 4199–4201 of TG-142. Daily checks should be done on equipment that can cause variations in delivered treatment doses.

[7] Not legally binding

For example output constancy, field sizes, optical distance indicators, safety interlocks and patient positioning lasers are recommended to be checked daily. Properties that could change over a month are done in the monthly tests. These include multiple tests for beam output and mechanical constancy. Laser guard-interlock and respiratory gating system test are recommended to be tested monthly.

The task group report TG-142 [22] suggests that a portion of the water phantom measurements, that were done during acceptance testing, should be repeated annually. Annual dosimetry test recommendations include tests for multiple field profile properties, beam quality and beam output constancy. Field symmetry and flatness measurements are included in the annual tests. A change of 1 % is the allowed change from baseline for both quantities. In safety tests the manufactures procedures should be followed. Mechanical tests, for example all rotational isocentres, should be checked annually. The annual measurements should be compared to the baseline measurements.

4.1.2 Reference dosimetry

Reference dosimetry (absolute dosimetry) means the traceability of the dose measurement to a primary standard. Primary standard dosimetry laboratories (PSDL) are designated for the purpose of developing, maintining and improving primary standards in radiation dosimetry. Secondary standard dosimetry laboratories (SSDL) use detectors that are calibrated against the PSDL and provide calibration services for example for radiation therapy clinics. IAEA have set recommendations on reference dosimetry in TRS398 (Technical Report Series) [23]. AAPM has also set instructions and guidance in TG-51 [24] and addendum WGTG-51 Report 374 [25]. Reference dosimetry is done in a water phantom with a cylindrical or plane parallel ionisation chamber. Water is used as the medium because its radiation absorption and scattering properties resemble that of tissues. Source-to-chamber distance (SCD) is set at 100 cm and field size to 10x10 cm^2 The calibration coefficients take different quantities into account.

Reference dosimetry measurements are done with calibrated detectors. The calibration need to have traceability to a PSDL. Different quantities need to be taken into account. Air temperature and pressure coefficient $k_{T,P}$ corrects for changes in the rooms conditions.

$$k_{T,P} = \frac{(273.2 + T)}{(273.2 + T_0)} \frac{P_0}{P} \tag{8}$$

In equation (8) T_0 and P_0 are normal air temperature and air pressure, which are commonly set to 20° C and 101.325 kPa. The current air temperature is T and air pressure is P.

Chamber polarity k_{pol} and voltage effects k_{elec} need to be accounted for also [1]. Polarity effects are caused by the opposite polarity of the ionisation chamber can cause measurement results to differ even in similar conditions. For megavoltage photon beams at the dose maximum depth chamber polarity effect can be neglected. In the buildup region the effect should be taken into account.

Chamber voltage effects are caused by the general and initial recombination as well as ionic diffusion loss. General recombination happens when opposite charges collide from different paths. If opposite charges on the same paths collide and recombine, initial recombination happens. In ionic diffusion loss charges diffuse against an electric field.

Equation (9) is used to calculate the dose absorbed dose in water $D_{w,Q}$.

$$D_{w,Q} = M_Q \cdot N_{D,w,Q_0} \cdot k_{Q,Q_0} \tag{9}$$

In equation (9) M_Q, is the corrected reading of the dosimeter. The quality factor of the reference beam is Q_0 and the quality of the measured beam is Q. Co-60 γ-ray beams are typically used as reference beams. Factor k_{Q,Q_0} corrects for the difference between the signal N_{D,w,Q_0} of the reference and measured beam. Beam qualities are evaluated with different methods for different beams. During the measurements linearity and effect, dose rate accuracy and dependence, constancy of output with gantry position, monitor chamber seal integrity, pressure and temperature compensation, collection efficiency and back-up counter should be monitored.

4.1.3 Relative dosimetry

Relative dose measurements do not require calibrated detectors or reference conditions. To be able to make comparison to previous measurements, a reference geometry is usually used in the measurements. Relative dosimetry is done by setting a fixed point, like the central axis, relative to other measurements.

For example PDD and profile measurements are relative dosimetry. Measurement can be done using both calibrated and uncalibrated detectors. PDD measurements are usually done by using a ionisation chamber (Section 3.1) in a water phantom.

Diodes (Section 3.4) and films (Section 3.5) can be used as well in relative dosimetry. In profile measurements, especially in determining the width of the penumbra films are more accurate than ionisation chamber measurements [18]. Diodes can only be used for relative dosimetry, because the sensitivity of the detector changes as it gets damaged by the radiation [1]. Diodes are used in *in vivo* dosimetry, because of their small size. *In vivo* dosimetry is done as an additional safeguard to make sure that there were no errors in the dose calculations. [16]

4.1.4 Acceptance testing

A new treatment machine goes through a preliminary calibration before it is allowed in patient use. AAPM has set detailed recommendations in TG-45 [21] and TG-142 [22]. For acceptance testing STUK Guide ST2.1 [20] gives similar recommendations on acceptance testing. The treatment rooms should have radiation warning sings and safety equipment installed. Also, warning lights and door interlocks with audio and video equipment for monitoring have to be installed into the rooms.

All personnel that work with the devices have to be trained. Acceptance testing is done together with user and vendor of the machine [20]. The dosimetric and mechanical should be within the units given by the vendor. These measurements also function as a baseline for future QA measurements. In Finland, before the radiation therapy machine can be used clinically, it needs to be inspected by STUK [4]. The inspection is done after the acceptance testing.

4.2 Radiation safety

Rooms that are used in radiation therapy need to have certain safety equipment to ensure patient and personnel safety. Treatment rooms have to have safety switches to cut the generation of radiation. Doors need to have interlocks to stop radiation production if someone opens a door into the room. When the treatment machine is on, there has to be warning lights or sound to warn about radiation generation. During treatments hospital personnel should have a video and audio connection to the treatment room. A door into the treatment room should be possible be opened from the inside of the bunker. [4]

By designing the room into a maze, the measured dose rates at the door can be lowered significantly. This reduces the amount of shielding needed at the door that

would otherwise be needed to reduce leakage from the room. Due to the neutron contamination of the photon beam at higher energies, shielding around the door of the room is important. [5, 26] Treatment rooms at TAUH use the maze design. Figure 16 shows a design of a treatment room at TAUH.

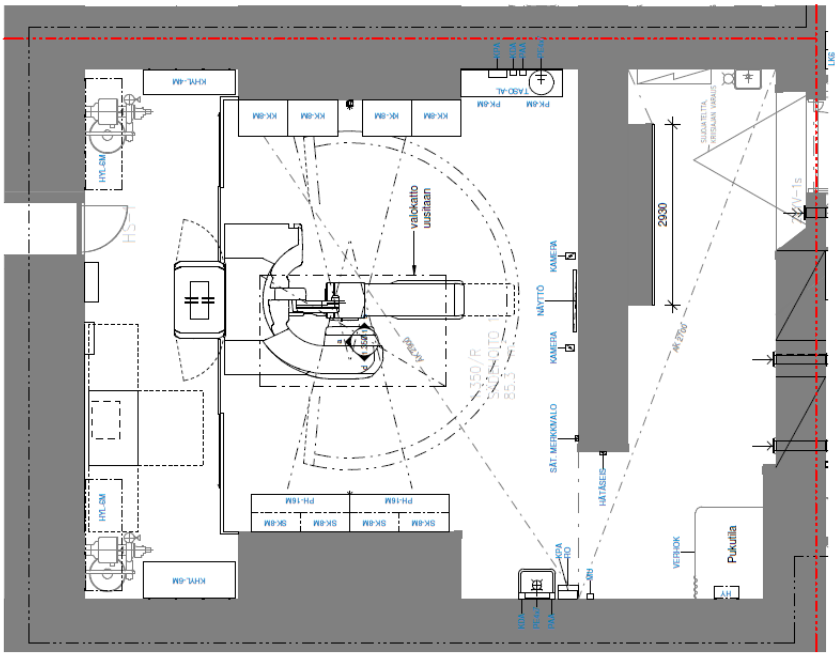

Figure 16. Radiation therapy treatment bunker design. The design is from a treatment room at TAUH that uses the maze design.

Dose rates have to be monitored in the areas where radiation is generated. In supervised areas, dose rates should not rise above 120 μSv/week and 6 μSv/week in unsupervised areas. Where the dose rates above 20 μSv/h, the personnel stay should be restricted and monitored. [4]

5 Methods and measurements

Photon beam profiles were measured for 6, 10 and 15 MV beams. Flattened profiles were measured for 6 and 15 MV beams and flattening filter free (FFF) were measured for 6 and 10 MV beams. TrueBeam v.2.7 (Varian Medical Systems, USA) linac was used in the measurements.

Ionisation chamber measurements were done in the BEAMSCAN (PTW) water phantom with Semiflex 3D (PTW) and Semiflex (PTW) chambers and MatriXX (IBA) array detector. Measurements were done with a 20x20 cm^2 field size. All the measurements were done with maximum allowed dose rates, which were 600 MU/min for 6 and 15 MV flattened beams and 2400 MU/min for 6 and 10 MV FFF photon beams, respectively. The measurements were repeated with a wedge (Figure 17) to cause a 5° change in the field symmetry. The wedge was home made by 3D printing.

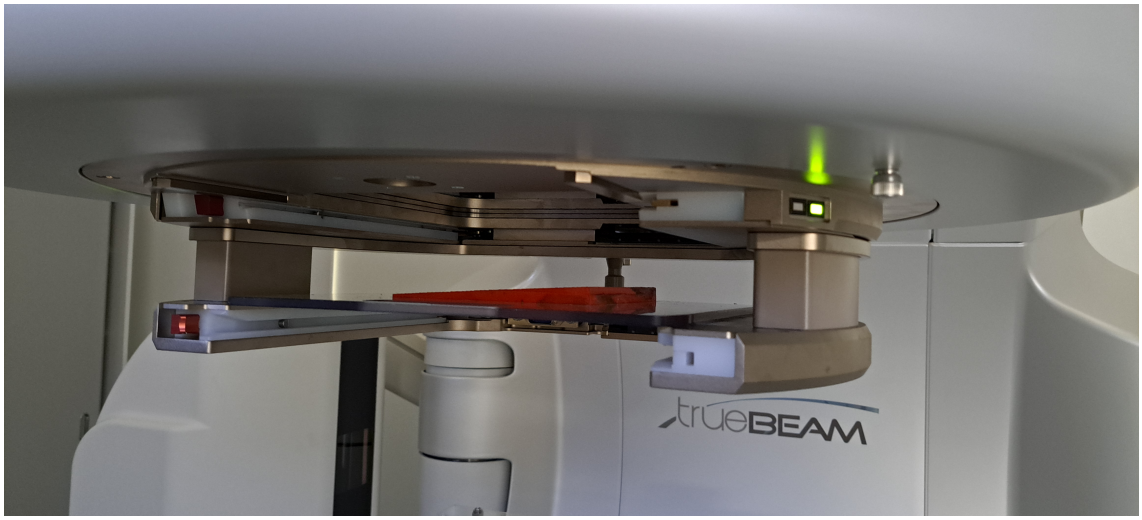

Figure 17. Wedge that was used to cause a change in the field profiles. The wedge was taped on to a holder that was attached to the treatment head. The angle of the wedge was 5 degrees.

5.1 Ionisation chamber measurements

BEAMSCAN (PTW) water phantom was used in the measurements. The tank was set-up so that the control unit and electrometer were towards the gantry (Figure 18). Before filling the phantom with water , the tank was levelled horizontally. White crosses on the walls of the tank were aligned with lasers. Because the phantom height could change when filled with water, the initial height from the laser line was marked with a pen on a piece of tape on the phantoms edge before filling with water.

The ionisation chamber positioning in the tank was done using Beamscan (PTW) phone application. In a reference run, the axes were calibrated by moving the detector to the four corners of the tank. After this the centre point of the field and SSD was checked and corrected using a SSD adjustment tool and a front pointer. SSD was set up to be 100 cm to the surface of water.

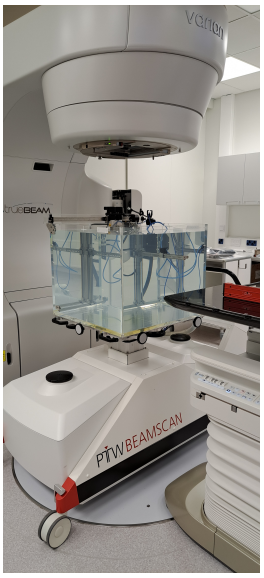

Figure 18. PTW BEAMSCAN water phantom set up under the gantry of the treatment machine.

Field detector and reference detector were set-up next. In the first set of measurements, both detectors were Semiflex 3D (PTW) Type 31021 (#142261) ionisation chambers. The chamber was submerged to 10 cm depth. The reference detector was kept in the at the corner of the treatment filed. The measurements were repeated in an open field with the Type 31021 Semiflex 3D (PTW) (#142261) and a Type 31010 Semiflex (PTW) (#007810).

Measuring was done in MEPHYSTO (PTW) software. Measuring and reference detectors were changed in the settings to be correct. Auto set up was run to calibrate tank axis to horizontal zero and centre to the radiation field.

Figure 19 shows the orientation of the ionisation chamber in the water phantom and the direction of movement in relation to the gantry. Crossline is the x-direction and inline is the y-direction.

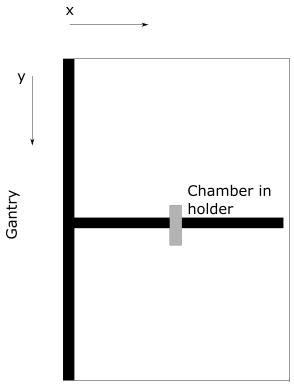

Figure 19. The ionisation chamber orientation in the water phantom. Ionisation chamber was in a holder in the water phantom. The holder was attached to the rail of the phantom.

5.1.1 Horizontal wire deep in water set up

At the time of the measurements, the QA program instructed to position the ionisation chamber positioned horizontally with the wire routed deep into the water phantom for profile measurements (Figure 20). The chamber was set in the horizontal position with the TRUFIX holder 150.

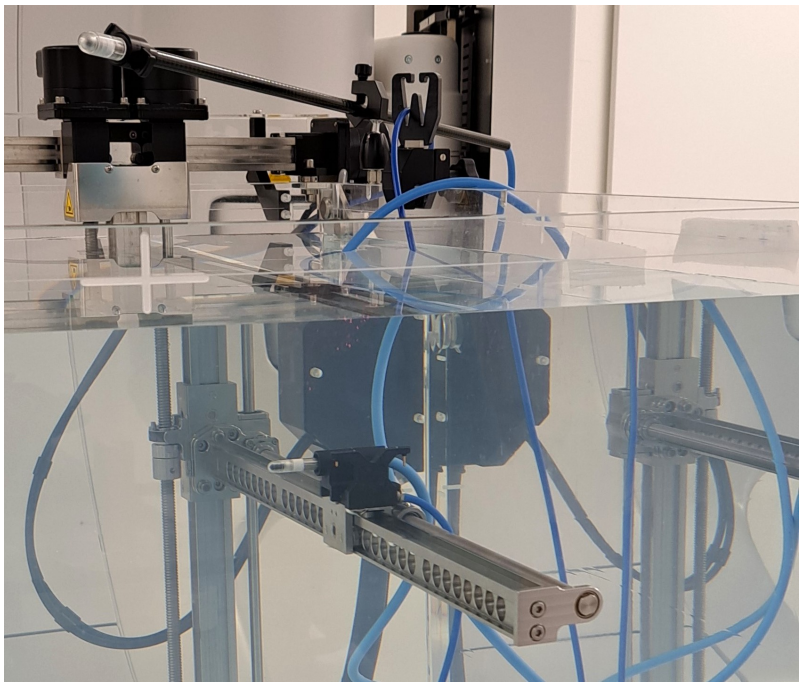

Figure 20. Horizontal positioning of the ionisation chamber. In the image the detector is at 10 cm depth with the wire deep in the water phantom.

5.1.2 Horizontal wire in field set up

In the second horizontal set up, the wire of the ionisation chamber was pulled closer to the surface of the water in the phantom (Figure 21) to see if this made a difference in the measured profiles. In this set up, the wire is more exposed to the radiation field.

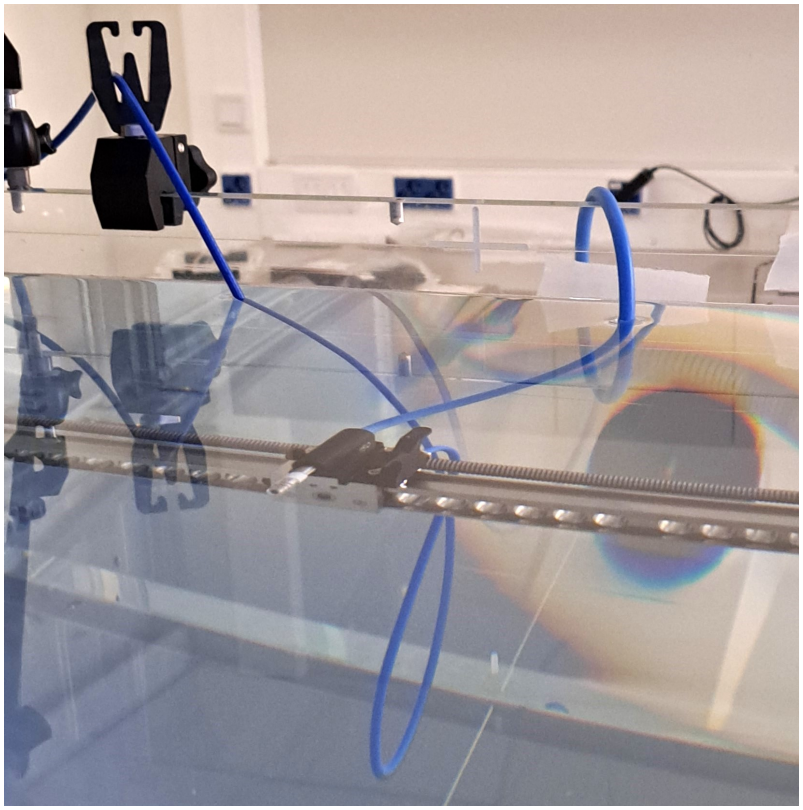

Figure 21. Horizontal positioning of the Semiflex 3D ionisation chamber with the wire closer to the surface of the water in the phantom.

5.1.3 Vertical set up

Third set up with the Semiflex 3D (PTW) was done with the chamber positioned vertically. For the vertical positioning TRUFIX holder 510 was used to position the detector vertically.

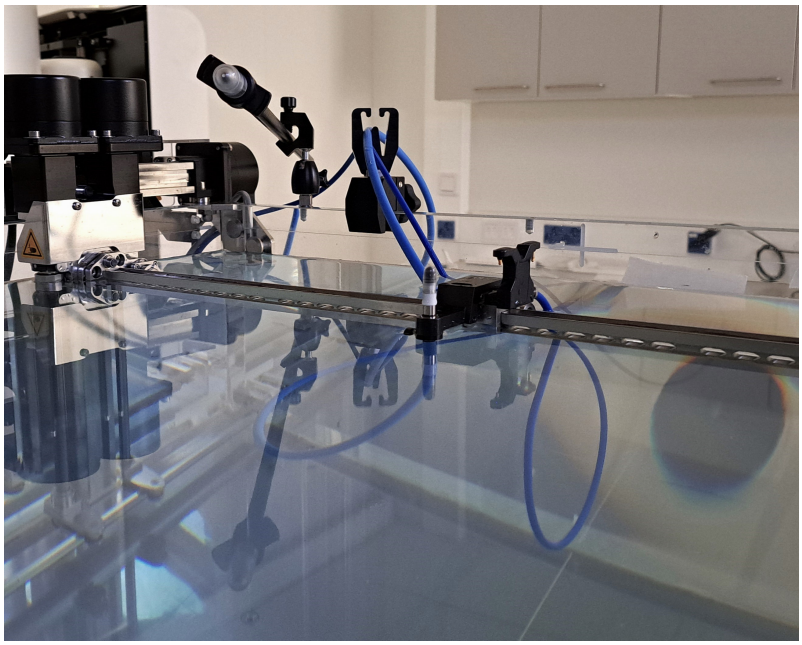

Figure 22. Ionisation chambers vertical positioning. The chamber is not submerged in the image.

5.2 Matrix detector measurements

MatriXX (IBA) was set up on the treatment table. Before measuring the detector needed to be warmed up to room temperature, which was done while the ionisation chamber measurements were taken. It was placed so that it was centred in the treatment field. The detector was centred with the alignment light of the machine. SSD was set at 100 cm again using the front pointer.

To simulate water above the measurement points, five 1 cm solid water plates were placed on top of the detector. The solid water plates are made of PMMA simulate the characteristics of water. The measurements were done with the detector inline with the gantry (Figure 23a). The measurements were repeated with the detector turned 90 degrees (Figure 23b).

myQA (IBA) software was used to take the measurements. In FastTrack mode of myQA, the matrix detector was pre-radiated and calibrated to the background radiation was measured in the treatment room before the measurements.

(a)

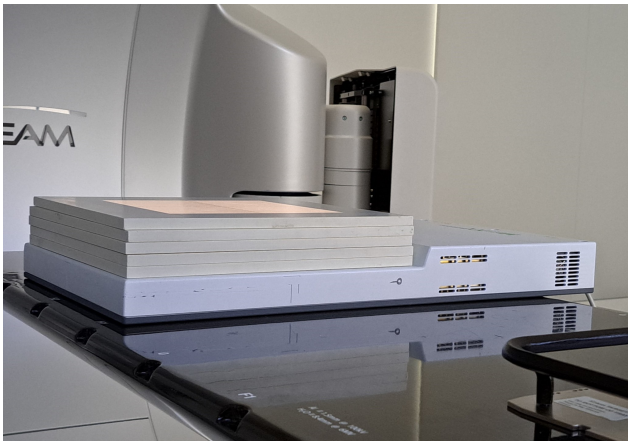

(b)

Figure 23. (a) Iba MatriXX measurement positioning inline with the gantry. The plates on top of the detector are dry water. Each plate is 1 cm thick. (b) With the matrix detector turned 90 degrees.

5.3 Analysis of the measurements

The measurements were analysed with Python. The flattened areas of the profiles were searched by interpolating the data on both sides of the central axis. An example profile with the interpolated points in the flattened field is shown in figure 24a. Symmetries were calculated afterwards using equation (3). Flatness values were calculated according to IEC protocols, using equation (4), for the flattened 6X and 15X photon beams. Flattened area was calculated for each field from the full width half max (FWHM) width of the beam using equation (10).

$$\text{Flattened area} = \text{FW} - 2(0.1 \cdot \text{FW}) \tag{10}$$

In equation (10), FW is the width of the field at the FWHM depth. The profiles were measured using 20x20 cm^2

Interpolation was also used to find the approximate 20 and 80 % dose points from the profile. The blue diamonds in the figure 24b below show the points that were used to calculate the penumbras on either side of the field.

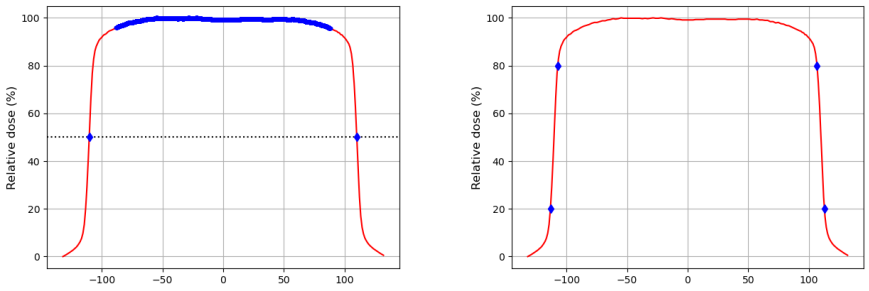

(a) **(b)**

Figure 24. (a) The blue dots show the flattened area in which symmetry and flatness of the field were calculated. Plot shows the FWHM points at 50 % dose depth, which was used as the field width in the flatness and symmetry calculations. (b) Figure shows the 20 and 80 % points that were used to calculate the left and right penumbras from the field.

6 Results

6.1 Field symmetry and flatness

Calculated symmetries from the measurements are shown in table 1. The measured fields had Semiflex 3D (PTW) significant differences in beam symmetries between the horizontal and vertical positioning. There were no significant differences between the wire deep in water and the wire in field set ups. The symmetries (Table 2) from the MatriXX (IBA) detector were inline with the horizontal Semiflex 3D (PTW) and the larger Semiflex (PTW) ionisation chamber.

Table 1. Calculated symmetries for the horizontally and vertically orientated Semiflex 3D (PTW) ionisation chamber.

Symmetry (x-axis)					
Horizontal Semiflex 3D (PTW)					
Set-up	Depth (cm)	6X	6FFF	10FFF	15X
Wire deep in water, Open	10	100.70	100.77	101.04	100.70
Wire in field, Open	10	100.70	100.79	101.05	100.70
Wire deep in water, Wedge	10	104.89	105.00	104.02	103.02
Wire in field, Wedge	10	104.68	104.90	104.12	103.01
Vertical Semiflex 3D (PTW)					
Set-up	Depth (cm)	6X	6FFF	10FFF	15X
Open	10	101.57	101.60	102.06	101.13
Wedge	10	105.76	106.23	105.09	103.68

Table 3 shows another set of measurements done with the Semiflex 3D (PTW) and with an larger Semiflex (PTW) in horizontal and vertical orientation. With the Semiflex (PTW) the difference in field symmetry between the horizontal and vertical orientations was smaller than with the Semiflex 3D (PTW). The older Semiflex (PTW) measurements had similar symmetries in both orientations as the vertical Semiflex 3D (PTW). The MatriXX (IBA) and Semiflex (PTW) measurements had similar profile symmetries in both orientations. The effect seen in the x-direction is

Table 2. The calculated symmetries from the MatriXX (IBA) detector measurements.

MatriXX (IBA)					
Symmetry (x-axis)					
Set-up	Depth (cm)	6X	6FFF	10FFF	15X
Open	5	101.77	101.01	100.60	101.10
Wedge	5	105.68	106.23	105.09	103.68
Rotation, Open	5	101.15	101.16	100.96	100.76
Rotation, Wedge	5	105.38	105.72	104.12	103.23
Symmetry (y-axis)					
Set-up	Depth (cm)	6X	6FFF	10FFF	15X
Open	5	100.28	100.26	101.06	100.81

not seen in the y-direction. Symmetry values were identical between the measurement set ups in the y-direction (Tables 3 and 2). This can also be seen from the plotted profile shown in appendix B.

Table 3. Second set of measurements comparing Semiflex and Semiflex 3D. Values are taken from the MEPHYSTO (PTW) software. Horizontal measurements were done according to the clinical QA program at TAUH.

Symmetry (x-axis)					
Set-up	Depth (cm)	6X	6FFF	10FFF	15X
Horizontal Semiflex 3D	10	100.70	100.69	100.83	100.70
Vertical Semiflex 3D	10	101.40	101.38	101.17	100.92
Horizontal Semiflex	10	101.26	101.44	101.23	101.06
Vertical Semiflex	10	101.46	101.50	101.15	100.98
Symmetry (y-axis)					
Set-up	Depth (cm)	6X	6FFF	10FFF	15X
Horizontal Semiflex 3D	10	100.63	100.49	100.96	100.58
Vertical Semiflex 3D	10	100.54	100.48	100.98	100.60
Horizontal Semiflex	10	100.54	100.57	100.91	100.54
Vertical Semiflex	10	100.60	100.51	100.93	100.69

Flatness values were calculated with the IEC protocol using equation (4) and were only calculated for the flattened 6X and 15X beams. The calculated values are presented in Table 4. With the Semiflex 3D (PTW) set up horizontally, the

calculated flatness values were similar with the wire in the water and with the wire out of the water tank for both beams. In the horizontal orientation, the flatness values differed by about 1% from the vertical Semiflex 3D (PTW) and the MatriXX (IBA).

Table 4. Calculated flatness values for the flattened 6X and 15X beams from the ionisation chamber data.

Flatness			
Horizontal Semiflex 3D (PTW)			
Set-up	Depth (cm)	6X	15X
Wire deep in water, Open	10	104.61	103.70
Wire in field, Open	10	104.60	103.70
Wire deep in water, Wedge	10	108.34	105.44
Wire in field, Wedge	10	108.31	105.31
Vertical Semiflex 3D (PTW)			
Set-up	Depth (cm)	6X	15X
Open	10	105.37	103.91
Wedge	10	109.20	105.84
MatriXX (IBA)			
Set-up	Depth (cm)	6X	15X
Open	5	102.77	104.63
Wedge	5	106.72	105.53
Rotation, Open	5	102.40	104.41
Rotation, Wedge	5	106.36	105.37

6.2 Left and right penumbras

The calculated widths of the penumbra on the left and right side of the field are presented in appendix F. In the flattened fields (Sections F.1 and F.4), when measured with the horizontal and vertical ionisation chamber, the penumbras on the left and right sides of the field were similar. The variation in the width of the penumbra between the left and right side was largest when measured with the MatriXX (IBA) detector. A known of cause of this is the low number of measurement points in the matrix detector in the region of the penumbra.

In the unflattened fields (Sections F.2 and F.3), the difference in the width the penumbra side to side was significantly less when measured with the ionisation chamber positioned horizontally. With the ionisation chamber in the vertical orientation and with the matrix detector the width of the penumbra on the left and right side of the field had a larger difference.

7 Discussion

To be able to meet the high criteria for radiation therapy treatment delivery accuracy, the beam quality needs to fulfil the set criteria for symmetry. In this study, it was shown that the horizontal orientaion of the small Semiflex 3D (PTW) chamber had significant effect on beam symmetry leading to possible mistuning the beam symmetry. The difference seen in the profile symmetries was around 1 %, when measured with the small Semiflex 3D (PTW) ionisation chamber in horizontal orientation and compared to other measurements. This may have significant effect on patient treatment if the profiles are measured wrong and tuned based on the wrong measurements.

The x-axial fields measured with the smaller Semiflex 3D (PTW) had similar symmetry and flatness values in the vertical orientation as the Semiflex (PTW) in both orientations. The cause for this is most likely that the less of the scattered particles from the water tanks parts are collected by the horizontal Semiflex 3D (PTW) because of its smaller size. Only the horizontal Semiflex 3D (PTW) deviated from the matrix detector. Orientation of the chamber was changed from horizontal to vertical in the QA program, so that the measurements are comparable with the larger Semiflex (PTW) chamber and MatriXX (IBA) detector. The the smaller ionisation chamber is preferred as it has a better measurement resolution.

In the BEAMSCAN (PTW) [27, p. 61] Hardware manual, PTW recommends using the chamber in the vertical orientation in relative dosimetry for the small Semiflex 3D (PTW) ionisation chamber. The manual says that "Irradiate the detectors axially, taking the measuring point shift into account". Because of the smaller size of the detector in the horizontal orientation the detectors measuring point is in a different spot than with the larger detectors. IAEA also has recommendations on the orientation of an ionisation chamber in TRS483, for reference dosimetry in small fields [17, p. 118]. IAEA recommends that "As with the use of any detectors that produce small signals, it is advised that care be taken in the detector orientation to minimize the effect of extra cameral current due to stem or cable signals".

In the future, a longer holder for the chamber could be tested to see how that

would affect the measurements. As the chamber would be further away from the rail on the water tank, it could decrease the number of scattered particles collected by the chamber.

The left and right side penumbras had big differences when measured with the MatriXX (IBA). Especially in the flattened fields rotating the detector 90° fixed this, which could be explained by positioning of the detector under the gantry. If the detector is misaligned by a millimetre, the measured field will have a significant difference in the penumbra, due to the low number of measurement points. With this known phenomena, matrix measurements are not used as such for penumbra measurement and are not directly comparable to ionisation chamber measurements. Matrix detector measurements can be used in routine checks to see the deviation from baseline measurements.

8 Conclusion

The vertical Semiflex 3D (PTW), Semiflex (PTW) and MatriXX (IBA) measured profile symmetry similarly. The horizontal Semiflex 3D (PTW) deviated from the other set ups. The orientation of the chamber was changed in the QA program due to this observation. Most likely the change in symmetry is caused by scattering from the water phantoms rails. This was confirmed as the change in symmetry was not seen in the y-axis profiles. Because of the higher measurement resolution of the Semiflex 3D (PTW) than the Semiflex (PTW), the clinic intends to do future beam profile measurements with the Semiflex 3D (PTW) ionisation chamber in vertical orientation.

References

[1] E. Podgorsak. *Radiation Oncology Physics: A Handbook for Teachers and Students*. Vienna: International Atomic Energy Agency (IAEA), 2005. ISBN: 92-0-107304-6.

[2] M. Tenhunen. *Sädehoidon fysiikka 1*. Fysiikan laitoksen luentomoniste. Helsinki, 2014.

[3] *Radiation act (859/2018)*. Helsinki, 2018. URL: https://www.stuklex.fi/en/ls/20180859#L13 (visited on 11/02/2022).

[4] *Säteilyturvakeskuksen määräys säteilylähteiden käytönaikaisesta säteilyturvallisuudesta ja säteilylähteiden ja käyttötilojen poistamisesta käytöstä (S/5/2019)*. Helsinki, 2019. URL: https://www.stuklex.fi/fi/maarays/stuk-s-5-2019 (visited on 11/02/2022).

[5] F. M. Khan and J. P. Gibbons. *The Physics of Radiation Therapy 5th Edition*. Philadelphia: Wolters Kluwer Health, 2014. ISBN: 978-1-4511-8245-3.

[6] R. Khabaz. "Effect of each component of a LINAC therapy head on neutron and photon spectra". In: *Applied Radiation and Isotopes* 139 (2018), pp. 40–45. DOI: /10.1016/j.apradiso.2018.04.022.

[7] C. Ma et al. "Flattening filter free in intensity-modulated radiotherapy (IMRT) - Theoretical modeling with delivery analysis". In: *Medical Physics* 46 (2019), pp. 34–44. DOI: /10.1002/mp.13267.

[8] D. Georg, T. Knöös, and B. McClean. "Current status and future perspective of flattening filter free photon beams". In: *American Association of Physicists in Medicine* 38(3) (2011), pp. 1280–1293. DOI: 10.1118/1.3554643.

[9] I. dosimetry. *OmniPro I'mRT System Version 1.7b - User's Guide*. 2010.

[10] A. Mahmoudi et al. "Penumbra reduction technique and factors affecting it in radiotherapy machines - Review study". In: *Radiation Physics and Chemistry* 157 (2019), pp. 22–27. DOI: /10.1016/j.radphyschem.2018.12.016.

[11] PTW. *Detectors for Ionizing Radiation - Including Codes of Practice*. 2022. URL: https://www.ptwdosimetry.com/fileadmin/user_upload/Online_Catalog/DETECTORS_Cat_en_16522900-14/blaetterkatalog/index.html#page_104d (visited on 04/14/2023).

[12] A. Kosunen et al. "Sädehoidon annosmittaukset: Ulkoisen sädehoidon suurenergisten fotoni- ja elektronisäteilykeilojen kalibrointi". In: (2005).

[13] PTW. *PTW BEAMSCAN brochure*. 2019. URL: https://www.ptwdosimetry.com/en/products/beamscan?downloadfile=1526&type=3451&cHash=5a80f78673024a479d62bdc440d8511d (visited on 04/14/2023).

[14] J. Herzen et al. "Dosimetric evaluation of a 2D pixel ionization chamber for implementation in clinical routine". In: *Physics in Medicine and Biology* 52 (2007), pp. 1197–1208. DOI: /10.1088/0031-9155/52/4/023.

[15] Y. Zhou et al. "A novel angular dependency model for MatriXX response and its application to true composite dose verification for IMRT plans". In: *Medical Physics* 22 (2021), pp. 120–135. DOI: /10.1002/acm2.13405.

[16] E. Yorke et al. "TG-62: Diode in vivo dosimetry for patients receiving external beam radiation therapy". In: (2005). DOI: 10.37206/88. URL: https://www.aapm.org/pubs/reports/RPT_87.pdf (visited on 12/09/2022).

[17] "Absorbed Dose Determination in External Beam Radiotherapy (TRS398)". In: (2017). URL: https://www-pub.iaea.org/MTCD/Publications/PDF/TRS398_scr.pdf (visited on 11/02/2022).

[18] S. Pai et al. "TG-69: Radiographic film for megavoltage beam dosimetry". In: (2007), pp. 2228–2258. DOI: /10.1118/1.2736779. URL: https://aapm.onlinelibrary.wiley.com/doi/full/10.1118/1.2736779 (visited on 12/08/2022).

[19] A. Niroomand-Rad et al. "Report of AAPM Task Group 235 Radiochrmic Film Dosimetry: An Update to TG-55". In: (2020), pp. 5986–6025. DOI: /10.1002/mp.14497. URL: https://aapm.onlinelibrary.wiley.com/doi/10.1002/mp.14497 (visited on 12/08/2022).

[20] *Design of rooms for radiation sources*. Helsinki, 2019. URL: https://www.stuklex.fi/en/ohje/ST2-1 (visited on 01/23/2022).

[21] R. Nath et al. “AAPM code of practice for radiotherapy accelerators: Report of AAPM Radiation Therapy Task Group No. 45”. In: (1994), pp. 1093–1121. DOI: /10.1118/1.597398. URL: https://aapm.onlinelibrary.wiley.com/doi/abs/10.1118/1.597398 (visited on 01/11/2023).

[22] E. E. Klein et al. “Task Group 142 report: Quality assurance of medical accelerators”. In: (2009), pp. 4197–4212. DOI: /10.1118/1.3190392. URL: https://aapm.onlinelibrary.wiley.com/doi/full/10.1118/1.3190392 (visited on 11/24/2022).

[23] “Absorbed Dose Determination in External Beam Radiotherapy (TRS398)”. In: (2000). URL: https://www-pub.iaea.org/MTCD/Publications/PDF/D483_web.pdf (visited on 11/02/2022).

[24] P. Almond et al. “AAPM’s TG-51 protocol for clinical reference dosimetry of high-energy photon and electron beams”. In: (1999). DOI: 10.1118/1.598691. URL: https://aapm.onlinelibrary.wiley.com/doi/epdf/10.1118/1.598691 (visited on 04/11/2023).

[25] B. Muir et al. “AAPM WGTG51 Report 374: Guidance for TG-51 reference dosimetry”. In: (2022). DOI: 10.1002/mp.15949. URL: https://www.aapm.org/pubs/reports/detail.asp?docid=227 (visited on 04/11/2023).

[26] *Safety in Radiotherapy*. Helsinki, 2019. URL: https://www.stuklex.fi/en/ohje/ST1-10 (visited on 01/23/2022).

[27] PTW. *BEAMSCAN Hardware - Operating Manual - Equipment Description*. 2019.

Appendices

A Horizontal Semiflex 3D (PTW) profiles at 10 cm depth (x-axis)

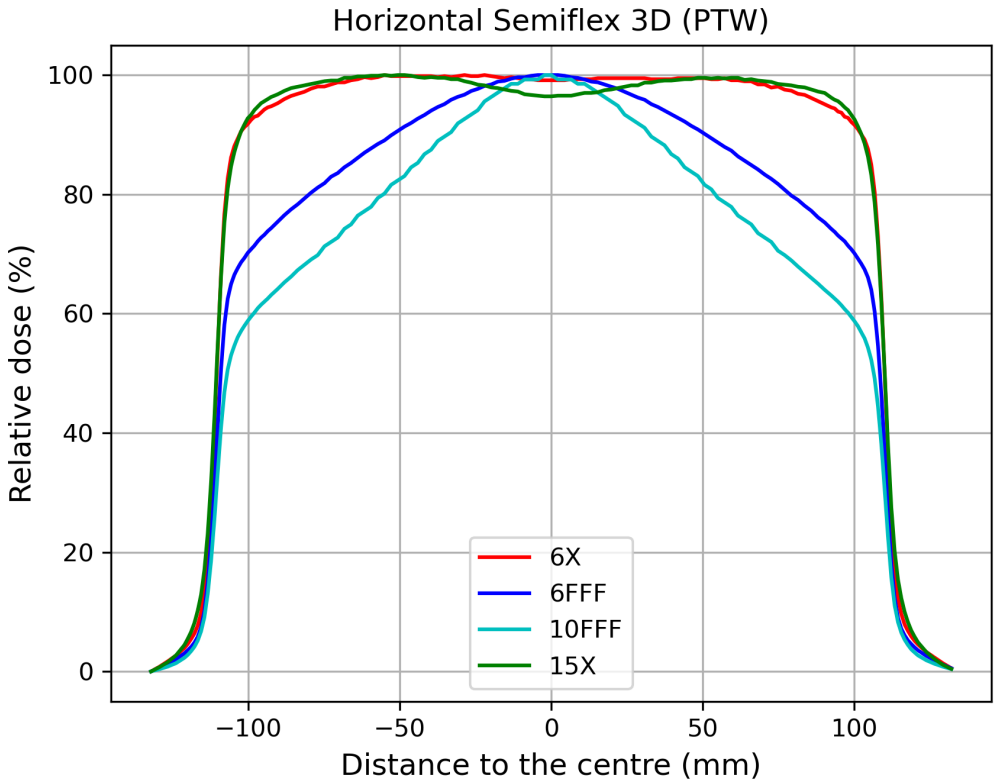

Figure 25. Beam profile with horizontal Semiflex 3D (PTW) with the wire submerged deep in the water.

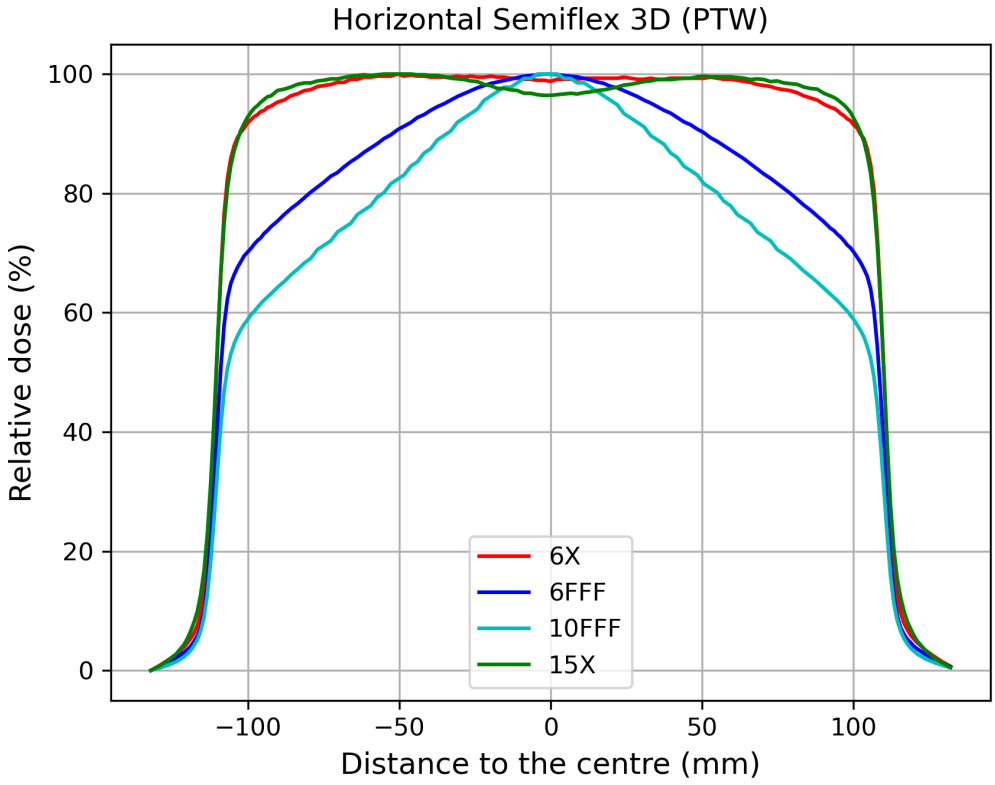

Figure 26. Profile for horizontally positioned Semiflex 3D (PTW) with the wire more in the field.

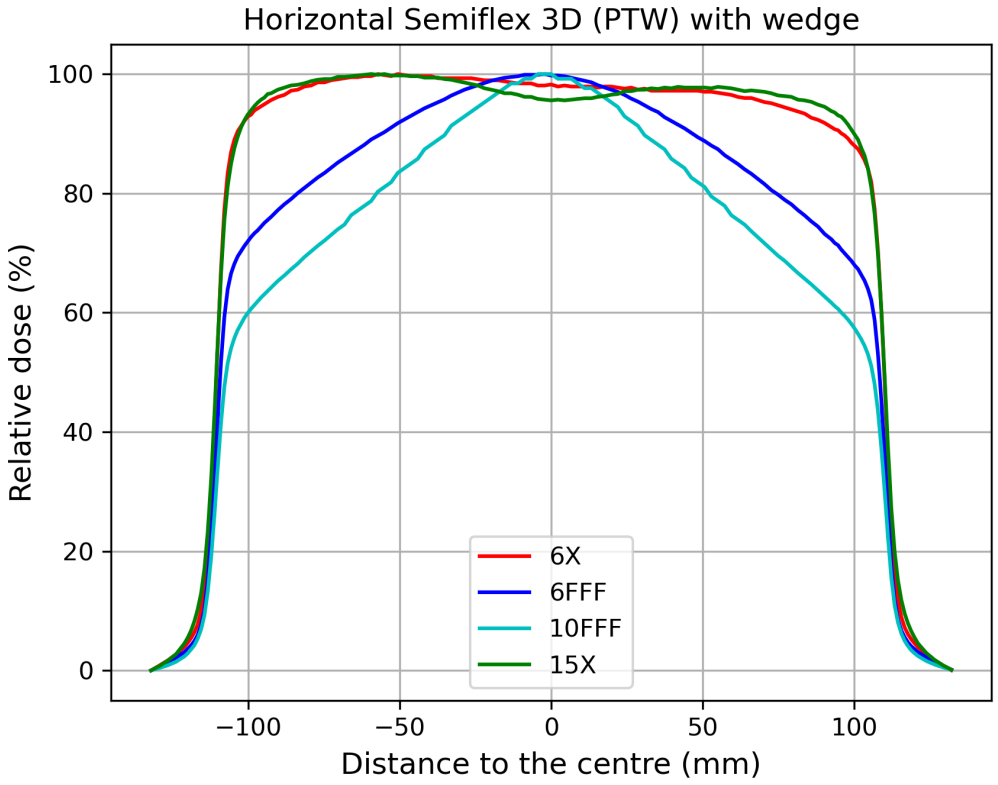

Figure 27. Profile for horizontal Semiflex 3D (PTW) with 5° wedge. With the wire deep in the water phantom.

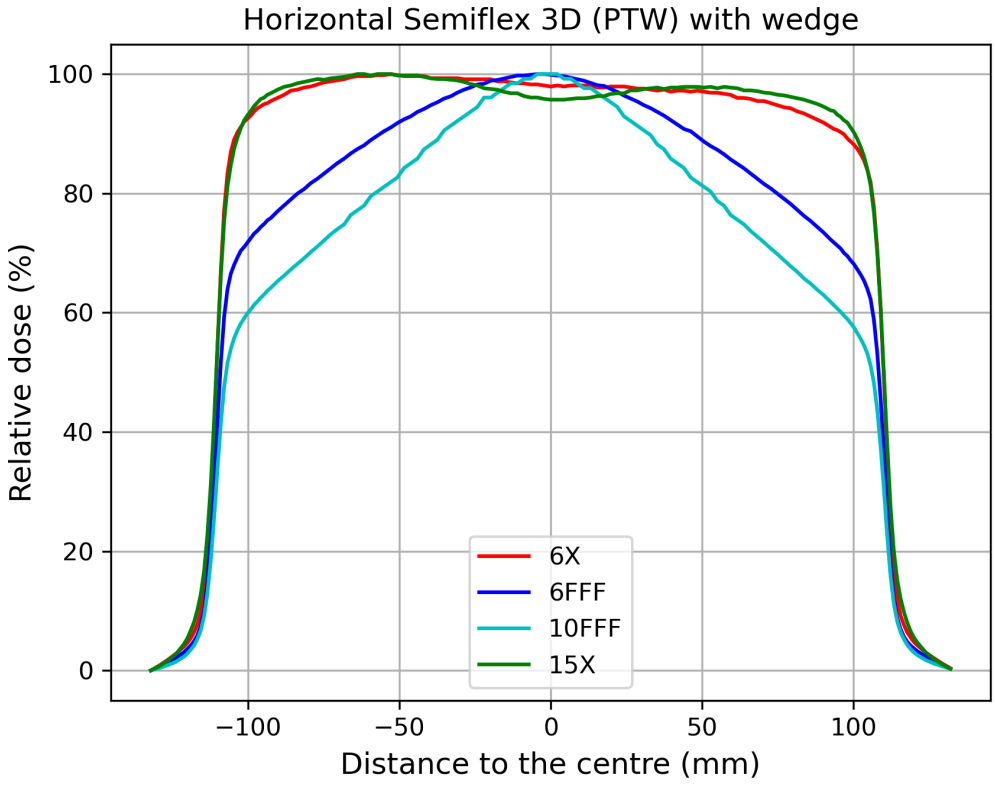

Figure 28. Profile for horizontal Semiflex 3D (PTW) with 5° wedge. With the wire more in the field.

B Horizontal Semiflex 3D (PTW) profile at 10 cm depth (y-axis)

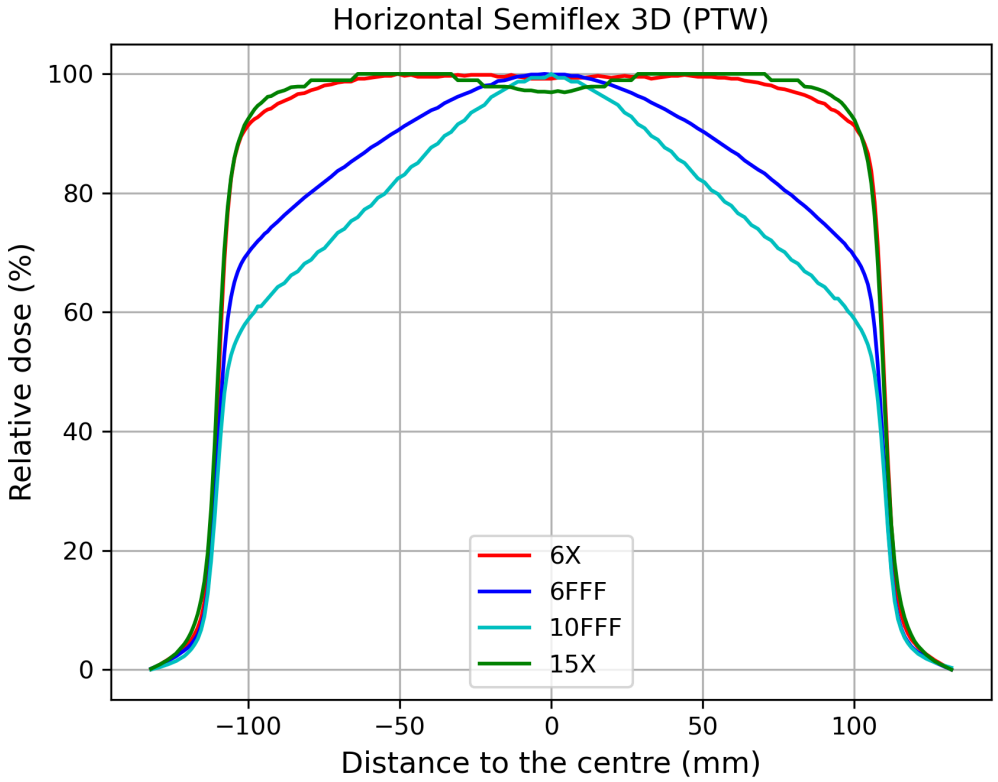

Figure 29. Y-axis directional profile with horizontal Semiflex 3D (PTW) with the wire deep in the water.

C Vertical Semiflex 3D (PTW) profiles at 10 cm depth (x-axis)

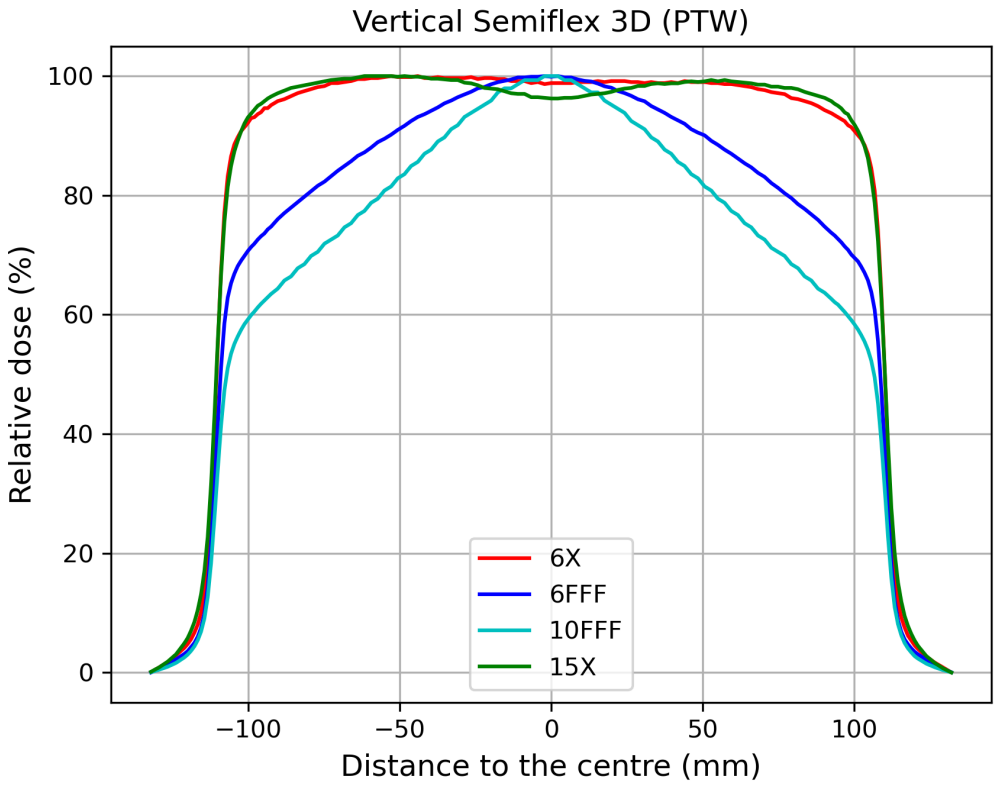

Figure 30. Beam profile for vertical Semiflex 3D (PTW)

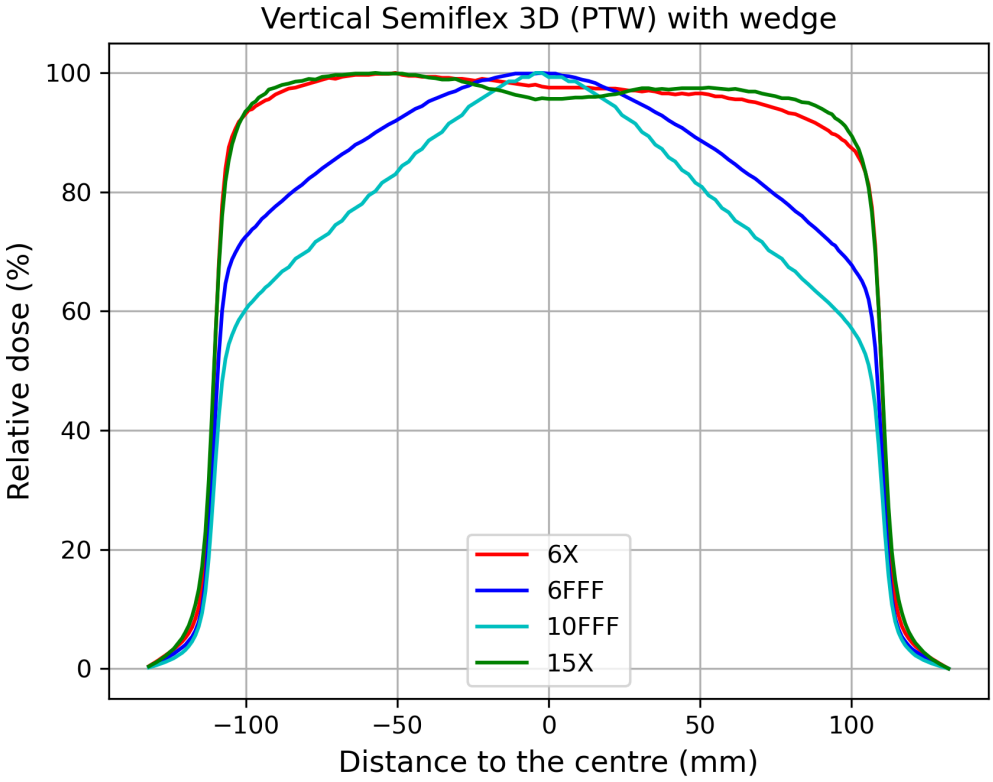

Figure 31. Beam profile for vertical Semiflex 3D (PTW) with 5° wedge

D MatriXX (IBA) profiles with 5 cm of solid water (x-axis)

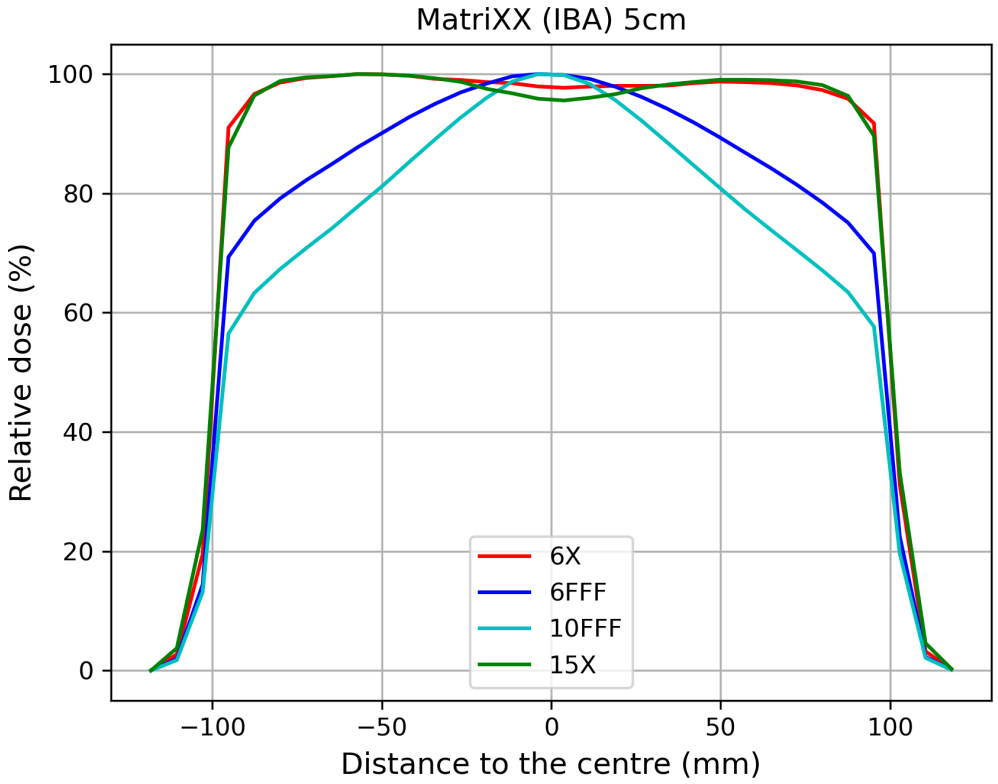

Figure 32. Beam profile with 5 cm of solid water on the detector.

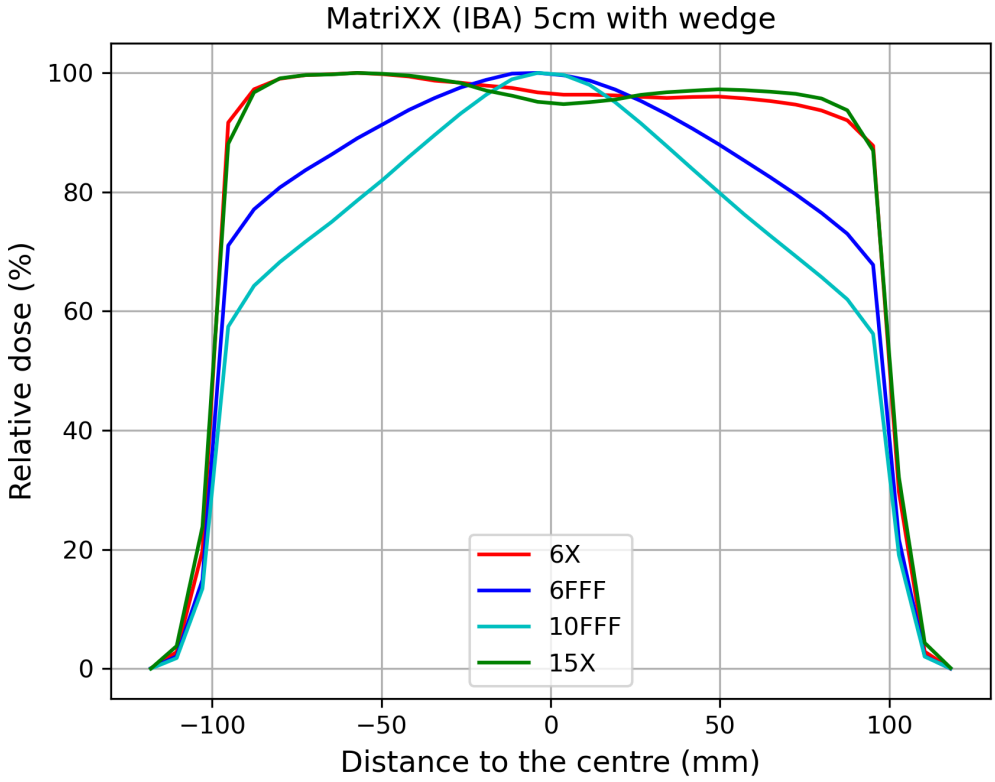

Figure 33. Beam profile with 5 cm of solid water and 5° wedge.

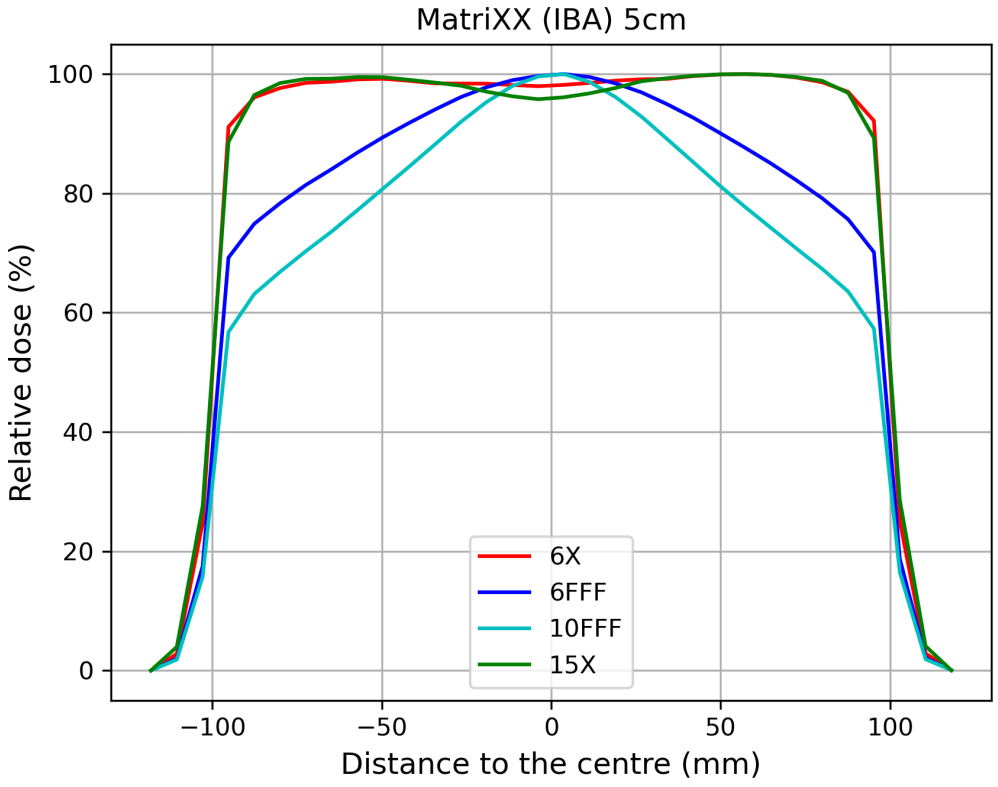

Figure 34. The detector was turned 90°. Measurement was done with 5 cm of solid water.

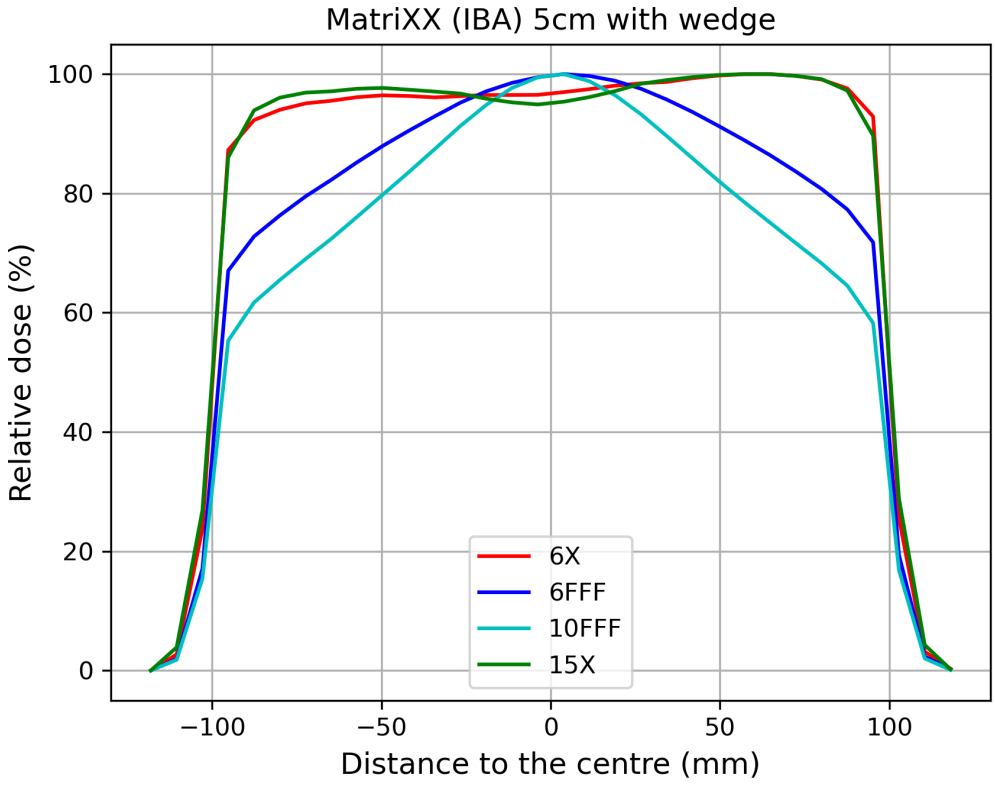

Figure 35. Beam profile with the MatriXX (IBA) turned 90°, with 5 cm of solid water and the 5° wedge.

E MatriXX (IBA) profile with 5 cm of solid water (y-axis)

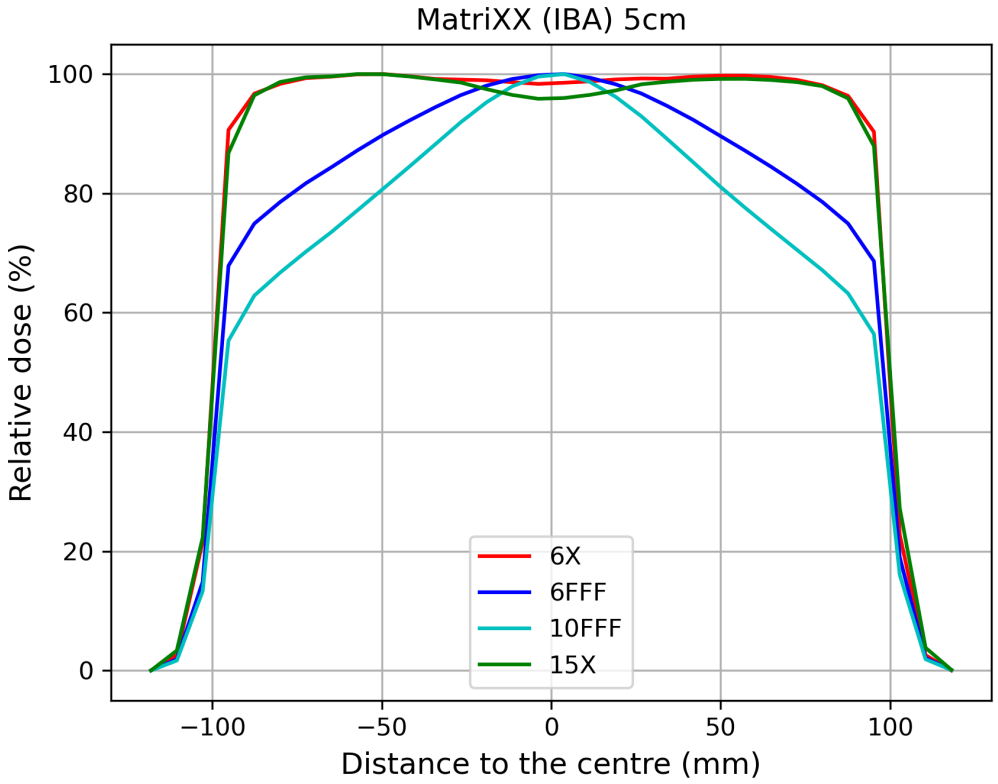

Figure 36. Beam profile with 5 cm of solid water on the detector.

F Calculated left and right penumbra widths

F.1 Penumbra widths for 6X beam

6X Penumbra				
Horizontal Semiflex 3D (PTW)				
Set-up	Depth (cm)	Left (mm)	Right (mm)	Difference (mm)
Wire deep in water, Open	10	6.09	6.12	0.03
Wire out of water, Open	10	6.10	6.11	0.01
Wire deep in water, Wedge	10	5.97	6.75	0.78
Wire out of water, Wedge	10	5.96	6.75	0.79
Vertical Semiflex 3D (PTW)				
Open	10	5.92	6.04	0.12
Wedge	10	5.85	6.82	0.97
MatriXX (IBA)				
Open	5	6.39	9.18	2.79
Wedge	5	6.36	9.35	2.99
Rotation, Open	5	7.98	7.98	0.05
Rotation, Wedge	5	8.10	8.05	2.63

F.2 Penumbra widths for 6FFF beam

6FFF Penumbra				
Horizontal Semiflex 3D (PTW)				
Set-up	Depth (cm)	Left (mm)	Right (mm)	Difference (mm)
Wire deep in water, Open	10	32.66	33.22	0.56
Wire out of water, Open	10	32.84	32.88	0.04
Wire deep in water, Wedge	10	28.87	37.73	8.86
Wire out of water, Wedge	10	29.02	37.24	8.22
Vertical Semiflex 3D (PTW)				
Open	10	31.55	34.03	2.47
Wedge	10	27.87	38.27	10.39
MatriXX (IBA)				
Open	5	24.23	27.69	3.46
Wedge	5	20.57	32.17	11.60
Rotation, Open	5	26.58	24.78	1.80
Rotation, Wedge	5	31.40	21.13	10.27

F.3 Penumbra widths for 10FFF beam

10FFF Penumbra				
Horizontal Semiflex 3D (PTW)				
Set-up	Depth (cm)	Left (mm)	Right (mm)	Difference (mm)
Wire deep in water, Open	10	56.59	57.44	0.85
Wire out of water, Open	10	56.56	56.34	0.22
Wire deep in water, Wedge	10	54.41	59.34	4.97
Wire out of water, Wedge	10	53.90	58.29	4.39
Vertical Semiflex 3D (PTW)				
Open	10	55.65	57.45	1.80
Wedge	10	54.35	59.54	5.29
MatriXX (IBA)				
Open	5	49.25	51.12	1.86
Wedge	5	47.68	53.08	5.40
Rotation, Open	5	50.79	49.77	1.02
Rotation, Wedge	5	52.84	48.24	4.60

F.4 Penumbra widths for 15X beam

15X Penumbra				
Horizontal Semiflex 3D (PTW)				
Set-up	Depth (cm)	Left (mm)	Right (mm)	Diff (mm)
Wire deep in water, Open	10	6.96	6.96	0.00
Wire out of water, Open	10	6.99	6.98	0.01
Wire deep in water, Wedge	10	6.91	7.44	0.53
Wire out of water, Wedge	10	6.91	7.36	0.45
Vertical Semiflex 3D (PTW)				
Open	10	6.86	6.92	0.06
Wedge	10	6.83	7.43	0.59
MatriXX (IBA)				
Open	5	8.09	9.83	1.74
Wedge	5	8.11	9.97	1.87
Rotation, Open	5	8.99	9.14	0.15
Rotation, Wedge	5	9.12	9.16	0.04